HHS Public Access

Author manuscript

Circulation. Author manuscript; available in PMC 2019 June 12.

Published in final edited form as:

Circulation. 2018 June 12; 137(24): 2613–2634. doi:10.1161/CIRCULATIONAHA.117.031046.

Cytosolic DNA Sensing Promotes Macrophage Transformation and Governs Myocardial Ischemic Injury

Dian Cao, MD, PhD[1,3,*], **Gabriele G. Schiattarella, MD**[1], **Elisa Villalobos, MSc**[1], **Nan Jiang, MSc**[1], **Herman I. May, BSc**[1], **Tuo Li, PhD**[2], **Zhijian J. Chen, PhD**[2,4], **Thomas G. Gillette, PhD**[1], and **Joseph A. Hill, MD, PhD**[1,2]

[1]Department of Internal Medicine (Cardiology), University of Texas Southwestern Medical Center, Dallas, TX 75390-8573, USA

[2]Department of Molecular Biology, University of Texas Southwestern Medical Center, Dallas, TX 75390-8573, USA

[3]VA North Texas Health System, University of Texas Southwestern Medical Center, Dallas, TX 75390-8573, USA

[4]Howard Hughes Medical Institute, University of Texas Southwestern Medical Center, Dallas, TX 75390-8573, USA

Abstract

Background—Myocardium irreversibly injured by ischemic stress must be efficiently repaired to maintain tissue integrity and contractile performance. Macrophages play critical roles in this process. These cells transform across a spectrum of phenotypes to accomplish diverse functions ranging from mediating the initial inflammatory responses that clear damaged tissue to subsequent reparative functions that help rebuild replacement tissue. Although macrophage transformation is crucial to myocardial repair, events governing this transformation are poorly understood.

Methods—Here, we set out to determine whether innate immune responses triggered by cytoplasmic DNA play a role.

Results—We report that ischemic myocardial injury, and the resulting release of nucleic acids, activates the recently described cGAS (GMP-AMP synthase)-STING (stimulator of interferon genes) pathway. Animals lacking cGAS display significantly improved early survival post-MI, diminished pathological remodeling including ventricular rupture, enhanced angiogenesis, and preserved ventricular contractile function. Furthermore, cGAS loss-of-function abolishes the induction of key inflammatory programs such as iNOS and promotes the transformation of

[*]To whom correspondence should be addressed at: Dian Cao, MD, PhD, Division of Cardiology, UT Southwestern Medical Center, 6000 Harry Hines Blvd, Dallas, TX 75390-8573, Tel: 1-214-648-1400, Fax: 1-214-648-1450, Twitter: @DrDianCao, dian.cao@utsouthwestern.edu or Joseph A. Hill, M.D., Ph.D., Division of Cardiology, UT Southwestern Medical Center, 6000 Harry Hines Blvd, NB11.200, Dallas, Texas, 75390-8573, Tel: 1-214-648-1400, Fax: 1-214-648-1450, Twitter: @josephahill, joseph.hill@utsouthwestern.edu.

DISCLOSURES

None

DATA SHARING

Data and resources will be made available upon request.

macrophages to a reparative phenotype, which results in enhanced repair and improved hemodynamic performance.

Conclusions—These results reveal, for the first time, that the cytosolic DNA receptor cGAS functions during cardiac ischemia as a pattern recognition receptor in the sterile immune response. Further, we report that this pathway governs macrophage transformation, thereby regulating post-injury cardiac repair. As modulators of this pathway are currently in clinical use, our findings raise the prospect of new treatment options to combat ischemic heart disease and its progression to heart failure.

Keywords

myocardial infarction; remodeling; macrophage; cGAS; cytosolc DNA

INTRODUCTION

Ischemic injury to the myocardium triggers a robust inflammatory response which is an integral part of the healing process and vital to maintenance of tissue integrity, preservation of contractile function, and optimal clinical outcomes.[1] This cascade of inflammatory events involves an initial destructive phase that serves to clear dead tissue. This, in turn, sets the stage for a subsequent repair phase that promotes myocardial healing.[2, 3]

While crucial to the repair process, the initial inflammatory response is closely associated with infarct expansion, myocardial rupture, and adverse remodeling in preclinical models[4] and in patients with acute coronary syndromes.[5–7] Although much effort has been directed at tempering the inflammatory response in hopes of achieving clinical gain, results from clinical trials have disappointed.[8] To date, major efforts have focused on individual cytokines, such as TNFα and IL1β, the complement cascade, and antibodies to adhesion molecules preventing leukocyte invasion (reviewed in [9]).

Macrophages are protagonists of both the inflammatory phase and the repair phase following tissue injury.[1] Initially, inflammatory monocytes/macrophages ($Ly6C^{hi}$ subtypes, M1-like macrophages) predominate within the infarct area.[10, 11] They elicit cytotoxic effector molecules such as ROS and NO, generate inflammatory cytokines such as TNFα and IL1β[12], and manifest avid phagocytic activity, thereby facilitating elimination of damaged myocardium and setting the stage for tissue repair. Subsequently, these $Ly6C^{hi}$ macrophages transform into a $Ly6C^{lo}$ subtype (reparative, M2-like macrophage) that fosters repair by promoting deposition of extracellular matrix proteins and angiogenesis and dampening inflammation through anti-inflammatory cytokines.[10, 12] Deficiency in this phenotypic transformation from destructive macrophages to reparative ones, as well as depletion of reparative macrophages, results in inefficient repair[13] and catastrophic outcomes after MI.[14]

The ability of macrophages to adopt a variety of functional phenotypes driven by subtle changes in microenvironmental cues makes them potential targets in modulating the inflammation process. In patients with an acute coronary syndrome, a dramatic spike in metabolic activity in the spleen likely reflects enhanced production of new monocytes which are ultimately recruited to the ischemic region[15] and are predictive of future events.[16]

Indeed, there is interest in targeting the macrophage transformation process in order to promote tissue repair and limit inflammation. However, better understanding of the environmental triggers and molecular networks regulating the switch of macrophage phenotype is required.

Damage to the myocardium resulting in cell injury and necrosis triggers both passive and active release of a variety of substances termed danger-associated molecular patterns (DAMPs).[17] These substances include proteins or protein fragments, small molecules, and RNA. These DAMPs, in turn, activate inflammatory mediators by binding to pattern recognition receptors (PRRs).[17] Although a number of DAMPs and PRRs have been identified as playing a role in the inflammatory response after MI[3], their roles in modulating macrophage function after ischemic injury remain poorly defined.

One possible but heretofore unexplored DAMP in myocardial injury is the DNA released by necrotic myocardium. We postulated that this cytosolic DNA is sensed by the cGAS-STING cascade, which thereby functions as a PRR in this context.[18] We go on to define the inflammatory events occurring downstream of this biology.

MATERIALS AND METHODS

All data, analytic methods, and study materials will be made available to other researchers for purposes of reproducing our results or replicating the procedures. Detailed methods are provided in the online data supplement.

Animals

Animals were maintained in a pathogen-free environment with free access to food and water. They were maintained on a 12-hour light/dark cycle from 6 am to 6 pm. All procedures were approved by the Institutional Animal Care and Use Committee at the University of Texas Southwestern Medical Center.

Statistical analyses

Findings are expressed as mean ± SD. The data were analyzed using statistical software (GraphPad Prism, version 7.01; GraphPad Software, San Diego, CA). An unpaired Student t test was performed to analyze 2 independent groups. One-way ANOVA coupled with the Tukey post-hoc test was used for pairwise comparisons. In representative datasets, we have also employed nonparametric tests (Wilcoxon rank sum test, Wilcoxon two-sample test, Kruskal-Wallis test). A value of $p < 0.05$ was considered statistically significant and results are depicted throughout as follows: *p<0.05; **p<0.01, ***p<0.001.

RESULTS

Myocardial infarction activates the cGAS-STING pathway

By sensing the presence of cytosolic DNA, the recently described cGAS-STING pathway plays a central role in the defense against microbial invasions.[18–21] After binding to cytosolic DNA, cGAS synthesizes a non-canonical second messenger, cyclic GAMP (cGAMP). cGAMP, in turn, activates STING, which then leads to the activation of interferon

regulatory factor 3 (IRF3)[22] that triggers expression of several genes, including type 1 interferon (IFN) and IFN-stimulated genes (ISG). IRF3 activates the core transcriptional programs induced by the prototypical stimulators of inflammatory macrophages, LPS and IFNγ[23, 24], serving to maintain their inflammatory activity.

Although massive cell death, with consequent release of both nuclear and mitochondrial DNA (nuDNA and mtDNA, respectively), is a central event in myocardial infarction (MI), whether this pathway participates in the resulting inflammatory response is unknown. To explore this, we began by assessing for activity of the cGAS-STING pathway after MI. Triggering of this pathway is gauged by transcriptional activation of a group of ISGs.[20, 25–28] ISGs are effector molecules of interferons and are responsible for their antiviral, anti-proliferative, and immunomodulatory effects.

We induced myocardial infarction by surgical ligation of the LAD coronary artery and collected samples at 3 and 7 days post-procedure. Using quantitative RT-PCR assays, we evaluated the abundance of transcripts coding for interferon-related factor 7 (*IRF7*), interferon-induced protein with tetratricopeptide repeat 1 (*IFIT1*), *IFIT3*, and *CXCL10*, all established to be transcriptional targets of cGAS-STING.[20, 25–28] We observed consistent and significant increases in *CXCL10, IFIT1, IFIT3*, and *IRF7* in mice post-MI as compared with sham-operated controls (Figures 1A–1D). Up-regulation of these markers occurred predominantly in the infarct zone and reached peak levels 7 days after coronary artery ligation. Consistent with the consensus in the literature that these are markers of cGAS activation, increases in these ISGs were not observed in *cGAS*$^{-/-}$ mice subjected to MI (Figures 1A–1D). Comparable findings were observed in bone marrow-derived macrophages (Figure S1). *CD14*, a macrophage surface receptor recognizing LDL and implicated in atherogenesis in humans[29–31] which has not been recognized as a target of cGAS activation, was also increased in *WT* mice subjected to MI but not in *cGAS*-null mice (Figure 1E), suggesting that *CD14* is under the control of this pathway as well.

In addition to detecting evidence of cGAS-STING pathway activation, we also observed significant increases in the abundance of transcripts coding for the pathway effectors themselves (Figures 1F, 1G). Up-regulation of STING was further confirmed at the protein level (Figures 1H, 1I), with increases occurring at a much lower magnitude in *cGAS*-null mice. Together, these findings point to cGAS-STING pathway activation in MI.

cGAS-mediated cytosolic DNA sensing during MI does not impact expression of major inflammatory cytokines

To begin to define effects of cGAS-mediated DNA sensing in MI, we first tested for changes in cytokine levels. The canonical molecular circuitry of cGAS-mediated DNA sensing is production of type I IFNs (IFNα and IFNβ) which are prototypical cytokines inducing inflammation in the setting of viral infection. In the context of myocardial ischemia, *IL1*, especially *IL1β*, is markedly induced and often linked with worse outcomes by promoting inflammation, remodeling, and heart failure.[4, 32, 33] That said, whereas pharmacological blockade of *IL1β* has met with recent success in atherosclerotic disease[34], in the context of myocardial remodeling from ischemic stress, this strategy has garnered mixed results.

[32, 35, 36] We observed that ischemic injury induced *IL1β* expression in the infarct region, as expected; however, inactivation of *cGAS* did not alter *IL1β* transcript levels (Figure 2A).

We next evaluated the inflammasome pathway, which is responsible for generating active *IL1β*. Again, we observed no differences between *WT* and *cGAS*$^{-/-}$ mice in the transcript levels of *caspase 1, IL18, and Nlrp3* (Figures 2B, 2C, 2D). Furthermore, loss of cGAS-mediated signaling did not alter *TNFα* and *IL6* (Figures 2E, 2F). Together, these results indicate that activation of the cGAS-STING pathway does not impact the major pro-inflammatory cytokines at the level of transcript abundance levels.

Cytosolic DNA-induced expression of M1 markers, iNOS, and Cxcl10, are cGAS dependent

We next turned our attention to macrophages. First, macrophages invade a myocardial infarction early, emerging as the majority cell type during and throughout the early phase of repair and peaking around day 6.[37] Our data pointing to activation of the cGAS-STING pathway (Figure 1) correlates largely with this time course. Further, macrophages harbor robust DNA-sensing activity.[20] Second, it is well established that M1 macrophages are pro-inflammatory and anti-microbial; M2 macrophages (also referred as reparative macrophages), on the other hand, are pro-wound healing, pro-fibrotic, and anti-inflammatory.[38] Further, ISGs under the control of cGAS (Figure 1) are among the most highly down-regulated genes during macrophage polarization from M1 to M2.[39] This, coupled with the established phagocytic nature of macrophages targeting damaged myocardium,[10, 40] suggested to us that cGAS-STING pathway activation may play a role in the transition of macrophage pools from an activated/inflammatory (M1-like) subtype to the activated/reparative (M2-like) subtype. To test this hypothesis, we harvested bone marrow-derived macrophages (BMDM) and evaluated their M1 versus M2 phenotype after they were challenged with DNA.

First, we evaluated the induction of inducible nitric oxide synthase (iNOS) and the expression of arginase 1 (Arg1). Nitric oxide (NO) mediates the cytotoxic effect of macrophages, and induction of iNOS is a signature of inflammatory macrophages.[41] Arg1 shares, and thus competes for, the same substrate (L-arginine) as iNOS. Arg1 metabolizes L-arginine into ornithine and proline, the latter being critical for the synthesis of collagen.[42] The macrophage dichotomy (M1 vs M2) originates in part from the divergent expression of iNOS and Arg1.[43, 44] As such, the ratio of iNOS to Arg1 is a classical readout in characterizing inflammatory versus reparative macrophages.

Transfection of ISD into WT BMDM resulted in a clear increase in (TANK)-binding kinase 1 (TBK1) phosphorylation (an established downstream element within the cGAS STING pathway) by 6 hours and which persisted for 24 hours (Figure 3A, 3B).[45] As expected this pathway was not activated in cells lacking cGAS (Figure 3A, 3B). Examination of Arg1 protein levels revealed no significant difference in the presence or absence of either ISD stimulation or cGAS ablation (Figure 3A, 3E). Conversely, ISD treatment resulted in a significant increase in iNOS levels only in *WT* cells (Figure 3A, 3C). Similarly, induction of CXCL10 by ISD was dependent on the presence of cGAS (Figure 3A, 3D). Finally, anti-inflammatory cytokines IL4 and TGFβ, which can counteract M1 activation,[46] reduced the levels of iNOS and CXCL10. Furthermore, *cGAS*-null macrophages expressed higher levels

of early *growth response protein 2* (*Egr2*), *fibronectin* (*Fn*), and *TGFβ* (Figure 3F), all of which participate in the molecular signature of M2 macrophages.[39] Also, DNA stimulation induced *CD38* expression exclusively in *WT* BMDM (Figure 3G). As *Egr2* and *CD38* are the most effective markers differentiating M1 and M2 macrophages,[39] these results lend further credence to a role for cGAS in the activation of inflammatory (M1) programs in macrophages.

cGAS is not required for the inflammatory response elicited by LPS and IFNγ

The inability of the cGAS-null BMDM to respond to ISD could be the result of a global defect in monocyte/macrophage differentiation or activation. As macrophages respond to a number of inflammatory signals, including lipopolysaccharide (LPS) and the cytokine interferon-γ, we next examined the impact of cGAS-mediated signaling in response to these polarizing agents. BMDM were treated with either LPS or INFγ and induction of the inflammatory response was measured. Unlike treatment with ISD, treatment with LPS and IFNγ elicited robust iNOS and Cxcl10 induction in both the WT and cGAS-null cells (Figure 3H, 3I). Similarly, a strong increase was noted in the mRNA levels of inflammatory cytokines, including *IL1β*, *IL1α*, and *IL6* in both WT and *cGAS*-null macrophages (Figure 3J). Additionally, ISGs, such as *IFIT1, IFIT3,* and *IRF7*, were induced by LPS and IFNγ similarly in *WT* and *cGAS*-null macrophages (Figure 3K). These data suggest that cGAS represents a novel pathway of macrophage activation distinct from LPS and IFNγ.

IL4 and TGFβ can act as M2 polarizing agents and both have been suggested to play positive roles in post-infarct repair.[14, 47] Baseline levels of the ISGs (IRF7, *IFIT1, IFIT3*) were reduced by treatment with these agents (Figure 3K). As these ISGs are downstream targets of cGAS-mediated signaling, their response to IL4 and TGFβ suggests a role in tissue repair after ischemia. The presence or absence of cGAS had no effect on the ability of LPS and IFN IFNγ to induce expression of ISGs in BMDM (Figure 3K).

cGAS$^{-/-}$ macrophages derived from human THP1 monocytes express higher levels of M2 markers and produce larger amounts of fibronectin

To determine whether a similar pathway of cGAS-mediated signaling occurs in human macrophages, we employed THP1 cells, a human monocyte cell line used extensively in macrophage-related research.[48–50] First, we engineered THP1 *cGAS*$^{-/-}$ cells using CRISPR-Cas9 technology (Figure S2A). Then, we differentiated the monocytes (THP1 *WT*, THP1 *cGAS*$^{-/-}$) into macrophages by incubating them with phorbol 12-myristate 13-acetate (PMA, 100 ng/mL, 48 hours)[51], followed by transfection of ISD to activate cGAS. We examined an array of markers used to distinguish M1 versus M2. As expected, transfection of ISD increased *IFNβ* expression exclusively in *WT* cells, confirming activation of the cGAS-STING pathway (Figure S2B). *CXCL10*, a downstream target of the cGAS-STING pathway and an M1 marker, expressed at a higher levels in *WT* cells at baseline and after ISD transfection as compared with *cGAS*-null THP1 cells (Figure S2C). In contrast, M2 markers, including *CD163, IL10*, and *CCL17*,[52, 53] were expressed at higher levels in THP1 *cGAS*$^{-/-}$ cells at baseline (Figures S2D, S2E, S2F). In response to ISD challenge, M2 markers did not manifest significant change in *WT* macrophages; however, there were further increases in *CD163, IL10*, and *CCL17* in *cGAS*$^{-/-}$ macrophages (Figures S2D, S2E,

S2F). These results suggest that the functional profile of these *WT* and *cGAS*$^{-/-}$ macrophages differ at baseline and in response to DNA stimulation.

Another characteristic of the M2 macrophage phenotype is increased production of fibronectin.[48, 53] A ligand of integrins αvβ3 and α5β1, fibronectin is enriched in the provisional matrix after MI[54, 55] and promotes cell adhesion and myofibroblast differentiation[56], a process central to myocardial wound healing.[57] To characterize further potential differences between THP1 *WT* and THP1 *cGAS*$^{-/-}$ cells, we examined fibronectin production in response to IFNγ, a classic stimulus that polarizes macrophages to M1,[53] and TGFβ and IL4, cues which elicit M2-like changes.[53] We were unable to use both IFNγ and LPS simultaneously for M1 polarization due to induction of cell death in THP1 *cGAS*$^{-/-}$ cells. THP1 cells manifested increased fibronectin expression in response to IL4 and IL13[48], the two classical cytokines used to polarize macrophages toward an M2 phenotype[53], and are thus classified as a M2 markers.[53] THP1 *cGAS*$^{-/-}$ macrophages produced markedly more baseline fibronectin, measured as the amount of fibronectin from total cellular protein samples as well as that secreted into the culture medium (Figures S2G, S2H). When stimulated with IFNγ, fibronectin levels decreased significantly in THP1 *cGAS*$^{-/-}$ cells, consistent with polarization toward the M1 subtype (Figures S2G, S2H). Regardless, THP1 *cGAS*$^{-/-}$ cells continued to produce significantly more fibronectin compared to *WT* (Figures S2G, S2H). TGFβ and IL4 treatment elicited an increase in fibronectin production in *WT* THP1 cells, but had no discernible impact in THP1 c*GAS*$^{-/-}$ cells (Figures S2G, S2H), suggesting that maximal production of fibronectin was present already. The inflammatory cytokine IL6, a marker of M1 macrophages[53], secreted into the medium in response to IFNγ by *cGAS*$^{-/-}$ THP1 cells was significantly lower than that from *WT* THP1 (Figures S2G, S2I).

Next, we investigated whether macrophages lacking *cGAS* can promote extracellular matrix protein synthesis in fibroblasts. Murine fibroblasts were co-cultured with WT or *cGAS*$^{-/-}$ macrophages derived from THP1 cells. After 48 hours of incubation, the fibroblasts were washed, collected and protein extracts prepared for Western analysis. We found that the steady state levels of fibronectin were significantly increased when fibroblasts were co-cultured with *cGAS*$^{-/-}$, but not WT, macrophages derived from THP1 cells (Figures S2J, S2K). Further, the levels of fibronectin induced in the fibroblasts decreased significantly when *cGAS*$^{-/-}$ macrophages were polarized toward the inflammatory subtype by exposure to IFNγ (Figures S2J, S2K).

Loss of cGAS signaling increases the abundance of reparative macrophages

Evidence presented so far suggests that loss of cGAS signaling promotes emergence of reparative M2-subtype macrophages. To test this in the setting of myocardial ischemia, transverse sections of hearts 6 days after myocardial infarction were stained for CD68 and CD206, cell surface markers commonly used to label total macrophages and the reparative M2 subtype, respectively. *WT* and *cGAS*$^{-/-}$ hearts harbored comparable total numbers of macrophages in the infarct region (Figure 4A). However, $CD68^{+}CD206^{+}$ macrophages were more prominent in the hearts of *cGAS*$^{-/-}$ mice, suggesting there are more reparative macrophages in the mutant animals (Figure 4A).

To further characterize the macrophage population after MI in *WT* and *cGAS*-null mice, we isolated immune cells from the infarct area and performed fluorescence-activated cell sorting (FACS) analysis. Cells were labeled with surface markers that differentiate them into myeloid cells, neutrophils, and macrophages/monocytes based on established gating strategies.[10, 13, 37]. The total macrophage/monocyte population was defined as $CD45.2^+Ly6G^-CD11b^+F4/80^+$ cells (Figure S3C). From this macrophage/monocyte population, subgroups of either $CD206^+$ or $CD206^-$ cells were further separated and quantified. $CD45.2^+Ly6G^-CD11b^+F4/80^+CD206^+$ cells represent the reparative M2 macrophage, and the $CD45.2^+Ly6G^-CD11b^+F4/80^+CD206^-$ cells represent the inflammatory M1 macrophage. In addition to CD206, we also examined subpopulations of macrophages based on either low or high levels of the cell surface marker Ly6C. $Ly6C^{high}$ macrophages are highly inflammatory and therefore are functionally in line with M1-like macrophages; in contrast, $Ly6C^{low}$ macrophages are primarily M2-like cells.

At baseline, the macrophage populations from *WT* and *cGAS*-null hearts were similar, comprising >90% $CD45.2^+Ly6G^-CD11b^+F4/80^+Ly6C^{low}$ cells (Figures S3A, S3B), a finding consistent with prior reports of WT cardiac-resident macrophages[37, 58] Three days after MI, the time point when macrophages begin to accumulate in the infarct region, the majority of macrophages were $CD45.2^+Ly6G^-CD11b^+F4/80^+CD206^-$ and $CD45.2^+Ly6G^-CD11b^+F4/80^+Ly6C^{high}$ cells in both *WT* and *cGAS*-null mice (Figure S3C, S3D, S3E), suggesting M1 inflammatory macrophages dominate the early stage of repair after MI in both genotypes. Six days after MI, however, we observed a significantly higher percentage of the $CD45.2^+Ly6G^-CD11b^+F4/80^+CD206^+$ in *cGAS*-knockout mice than in *WT*, 54% versus 29% ($p<0.05$), respectively (Figures 4B, 4C).[1] Furthermore, the macrophage population from *cGAS*-null hearts post-MI harbored higher percentages of $CD45.2^+Ly6G^-CD11b^+F4/80^+ Ly6C^{low}$ cells but fewer $CD45.2^+Ly6G^-CD11b^+F4/80^+ Ly6C^{high}$ macrophages (Figures 4B, 4D), consistent with a more abundant M2-like population. We observed no significant differences in the number of total macrophages at day 3 post-MI after adjusting for the volume of infarct tissue, suggesting that cGAS does not play a major role in maintaining the total population of macrophages at this time point. In aggregate, complementary data collected from both immunohistochemistry and FACS analyses demonstrate that *cGAS* silencing results in significantly more abundant reparative macrophages in the infarct zone of LV.

Loss of cGAS signaling facilitates myocardial wound repair by promoting myofibroblast transformation and angiogenesis

Reparative macrophages have been suggested to promote wound healing in hearts damaged by myocardial ischemia, although the exact mechanism is not well defined.[10, 13, 14, 59] Efficient repair depends on the transformation of fibroblasts into myofibroblasts which produce copious amount of extracellular matrix protein and facilitate wound contraction,[60] processes essential in building replacement tissue with high tensile strength in order to prevent infarct expansion and rupture. To determine the impact of cGAS silencing on fibroblast differentiation after cardiac ischemic injury, we performed immunohistochemical staining for αSMA (α-smooth muscle actin) (Figure 4E), a commonly used marker of myofibroblasts.[61] We detected significantly stronger and more extensive αSMA staining in

the infarct border and central areas of *cGAS*$^{-/-}$ hearts compared with *WT* (Figure 4E), suggesting that myofibroblasts are more prevalent in knockout hearts during the process of myocardial wound repair.

Macrophages and specifically M2-like macrophages play key roles in promoting angiogenesis in tumors.[62, 63] Given this, we next tested for effects of the observed M2-like cells switch on neo-vascularization in *WT* and *cGAS*-null mice after MI, labelling heart sections with CD31, an endothelial cell surface marker. At baseline, vascularization was similar in *WT* and *cGAS*-null hearts (Figure S4). However, in heart tissue after MI we detected remarkably more microvasculature in *cGAS*-null mice hearts after MI compared to *WT* (Figure 4F). This difference was most apparent in the border and center region, with no significant differences seen in the remote region. In aggregate, these results support a model in which cGAS-mediated signaling in MI induces M1 inflammatory macrophages and that suppression of this pathway leads to sequela consistent with M2 reparative macrophages.

Inactivation of cGAS diminishes pathological ventricular remodeling post-MI and improves survival

Findings reported thus far demonstrate that cGAS-dependent sensing of cytosolic DNA promotes a phenotypic shift toward the inflammatory, M1-like macrophage subtype. In the absence of cGAS, phenotypically M2-like cells predominate promoting wound healing phenotypes such as enhanced fibrogenesis and angiogenesis. Given this, we postulated that loss of cGAS signaling would blunt pathological remodeling in the setting of MI. After confirming that areas at risk of infarction were comparable in the two genotypes (Figure S5), we subjected *WT* and *cGAS*-null mice to myocardial infarction and evaluated a panel of molecular, morphological, and functional parameters over a time span of 3 days (acute), 2 weeks (subacute) and 3 months (chronic). First, transverse sections of the left ventricle were evaluated at the level of LAD ligation and 0.5, 1.0, 1.5, 2.0, and 2.5 mm below the ligation (Figures 5A, 5B).

We first observed that chamber dilation and infarct expansion were significantly attenuated in *cGAS*$^{-/-}$ hearts. Gravimetric analyses revealed that heart weight normalized to body weights (HrtW/BW) or tibia length (HrtW/TL) were greater in *WT* animals than in *cGAS*$^{-/-}$ mice (Figure 5C, 5D). We observed statistically significant differences as early as 3 days post-MI, the earliest time point studied, and the those differences persisted at 7 and 14 days. Geometric remodeling index (GRI, LV cavity area divided by the thickness of the septum), an index of LV geometry, manifested wide separation between *WT* and *cGAS*$^{-/-}$ mice (Figure 5E). The progressive increase in GRI towards the apex is consistent with greater chamber enlargement distal to the LAD ligation in *WT* animals due to infarct expansion. Notably, this progressive increase in GRI was not observed in *cGAS* knockout mice, suggesting diminished infarct expansion and less LV dilatation.

Cardiac mass continued to increase during the chronic remodeling phase in *W*T mice (12-week post MI), but this trend was blunted in *cGAS* knockout animals (Figure 5F). Further, whereas baseline echocardiographic parameters were comparable in *WT* and *cGAS*-null mice (Table 1), contractile function measured 10-week post-MI was significantly improved in *cGAS* knockout hearts compared to *WT* (Figure 5G).

To characterize the remodeling process further, we evaluated activation of the fetal gene program post-MI in *WT* and *cGAS* knockout mice. We noted that these markers of pathological ventricular remodeling were significantly lower in *cGAS* knockout hearts (Figures 5H, 5I, 5J, 5K).

In order to determine whether cGAS deficiency impacts infarct size, we employed the midline method as described.[64] The percentage of scar length to LV circumference drawn midway between epicardial and endocardial surfaces is a validated measure of infarct size, one which is more accurate than scar area owing to scar thinning which can lead to under-estimation of infarct size.[64] When comparing infarct sizes on serial LV cross sections, we observed a modest decrease in infarct size in *cGAS*-null mice, especially at the basal sections (Figure 5L). Remarkably, however, silencing of *cGAS* led to robust improvement in post-MI survival (Figure 5M): mortality within 1 week of MI was 42% (15 out of 35) in *WT*, comparable to that reported as 25%–42% in the literature.[14] Mortality in *cGAS*-null mice, however was 3% (Figure 5M) ($p<0.001$).

Post-mortem examination revealed that the major cause of post-MI mortality was free wall rupture, as illustrated in a section from a *WT* mouse (Figure 5N), followed by heart failure. Again, these relative proportions leading to death are consistent with those reported in the literature.[14] Our finding of low mortality in *cGAS*-null mice is consistent with improved myocardial wound healing leading to the formation of replacement tissue with greater tensile strength. Equally or more important, inadequate repair imposes greater hemodynamic stress on the remaining normal myocardium and exacerbates remodeling that occurs acutely within one week of MI.[65] Collectively, our data are consistent with a model in which the cGAS-mediated cytosolic DNA sensing pathway inhibits post-infarction repair and the major benefit accrued from loss of cGAS signaling stems from improvement in maintenance of tissue integrity and diminished remodeling, commencing early in the acute stage and lasting well into the chronic phase.

Blocking cGAS-mediated DNA sensing improves myocardial repair after infarction

To define mechanisms underlying the robust improvement in cardiac structure and function post-MI in *cGAS*-null animals, we tested for evidence of enhanced post-injury repair. First, we assessed the infarct region for collagen deposition. Hematoxylin-eosin staining 1-week post-MI at the border and the central regions of the infarct revealed that general cellular infiltration was similar in *WT* and *cGAS*-null hearts (Figure 6A). However, the infarct region in $cGAS^{-/-}$ mice at both areas was denser with more compact architecture compared with *WT* animals. We then analyzed collagen content using Masson's trichrome (TC) staining, picrosirius red (PSR) staining, and polarized light (PL). Trichrome and picrosirius red staining are standard methods used to quantify collagen content in tissues[14, 66, 67], and polarized light detects the natural birefringence of collagen and provides additional information of collagen fiber structure, order, thickness, and packing.[66, 68] Both trichrome and picrosirius red staining revealed denser collagen deposition in $cGAS^{-/-}$ hearts (Figure 6B). Under polarized light, collagen was detected in a tightly packed, multi-molecular microfibrillar form in *cGAS* knockouts, whereas it appeared as single fibers in *WT* animals (Figure 6B). Signal quantification using ImageJ software, presented as percentage of

collagen-occupying area relative to the total area of each microscopic field, revealed that collagen density increased to 41.7±4.7% (by TC), 42.9±5.5% (by PSR), and 36.1±6.1% (by PL) in *cGAS*$^{-/-}$ hearts (Figures 6C, 6E). Conversely, collagen density in *WT* infarct was 26.7±5.7% (by TC), 29.3±5.3% (by PSR,) and 25.7±3.4% (by PL) ($p<0.001$ for each of the three quantitative methods), values which are similar to those reported in the literature.[14]

To directly compare the amount of collagen localized within the ischemic region, we purified soluble and insoluble collagen from *WT* and cGAS-null mice one week post-MI and quantified collagen levels. We found a significantly greater abundance of soluble collagen in the provisional matrix in *cGAS*-null mice, whereas the insoluble fraction of collagen was comparable between *WT* and *cGAS*-mutant mice (Figure 6F). As insoluble collagen is extensively cross linked, these data suggest that the collagen in *cGAS*-null mice after MI has not yet cross-linked extensively, consistent with the early stage of repair at one week. These results, nonetheless, support the notion that *cGAS* silencing leads to a higher collagen concentration in the infarct region.

The presence of dense granular tissue, higher density collagen, and more collagen fibrils suggest that tensile strength from the healing tissue in *cGAS* knockout animal hearts is greater than that in *WT*. To test the notion that hemodynamic stress in the remote region of the ventricle was mitigated in *cGAS*$^{-/-}$ hearts, we compared collagen 1 and fibronectin levels from remote tissue areas after MI (Figures 6G, 6H). Collagen 1 content was significantly greater in the remote area of *WT* heart than in a similar area in *cGAS*$^{-/-}$ hearts three days after MI. At the same time point, fibronectin levels were also more abundant in *WT* hearts than in *cGAS*$^{-/-}$ hearts. Increases in collagen 1 subsided after 1 week, whereas fibronectin remained elevated in *WT* but not *cGAS*$^{-/-}$ hearts (Figures 6I, 6J). As the major ECM proteins, increases in collagen 1 and fibronectin represent immediate ECM expansion in the non-infarct area, a phenomenon also observed clinically after MI.[65] As the increase in ECM content is a sequela of hemodynamic stress and systolic dysfunction, reduced collagen 1 and fibronectin levels in *cGAS*$^{-/-}$ mice suggest more favorable hemodynamics and better systolic performance in the non-infarcted myocardium. In aggregate, these findings point consistently to enhanced tissue repair after ischemic damage in *cGAS*-null mice.

Evidence of cGAS-STING pathway activation in human heart failure samples

Finally, to begin to evaluate the relevance of these findings in human disease, we tested for activation of the cGAS-STING pathway in human heart failure secondary to ischemic heart disease. We obtained heart tissues from both failing and non-failing hearts from the Duke Human Heart Repository (baseline clinical characteristics are provided in Table 2). RNA was harvested from normal control hearts, from failing hearts at the time of LVAD implantation, and from the same patients post-LVAD at the time of heart transplantation surgery. Consistent with our findings in mice, dynamic changes in the abundance of *cGAS* and its target *CXCL10* transcripts were seen before and after LV unloading (Figures 7A, 7B), suggesting strongly that this pathway is active in clinical heart failure in patients.

DISCUSSION

Inflammatory mechanisms play a central role in the response to myocardial ischemic injury. Cell injury triggers the release of DAMPs which bind to PRRs, triggering inflammatory responses. The sterile inflammation that ensues is critical to the repair of the initial insult. However, overheated inflammation eventually leads to disease. Among the mechanisms leading to resolution of injury, macrophage-dependent clearance of necrotic tissue followed by tissue repair is vital,[10, 13, 14, 69] and macrophage transformation from inflammatory cells to a reparative phenotype is the prerequisite for tissue healing. However, the environmental cues and mechanisms governing the shift from the destructive M1 macrophage phenotype to the reparative M2 subtype have remained obscure. Here, we explored the role of a recently described innate immune pathway of cytosolic DNA sensing. We report that the cytosolic DNA sensor cGAS is activated robustly in the setting of myocardial infarction, triggering downstream events mediated by the STING cascade. This, in turn, promotes macrophage transformation toward the M1-like subtype. Inactivation of this pathway promotes transformation toward the M2-like macrophage subtype, facilitating wound healing, angiogenesis, diminished pathological cardiac remodeling including ventricular rupture, and markedly enhanced survival post-MI. Together, these findings point to cGAS as a PRR for ischemic injury and uncover a novel mechanism that governs macrophage phenotypic switching and post-infarction remodeling.

Post-MI ventricular remodeling

The tissue wound stemming from myocardial infarction is most vulnerable between days 2 and 7 post-MI, when tissue destruction is robust and only granular tissue, but not scar with high content of mature collagen, is present. This leaves the left ventricular free wall prone to rupture, and due to compromised capacity to generate tension, progressive thinning of the infarct region and increased hemodynamic stress in remote tissue zones. In fact, in murine MI models, rupture is the predominant cause of death.[70] Cardiac rupture, although less common in MI patients presently, remains an important concern, accounting for 12.4% of deaths in patients enrolled in the VALIANT trial published in 2010.[71]

Ischemic injury of the myocardium triggers a complex cascade of events involving clearance of necrotic tissue, deposition of extracellular matrix elements, and tissue repair.[3] The extent of the initial infarction and effectiveness of the repair process after this event combine to dictate long-term ramifications on heart function. Clinically, limiting infarct size by timely reperfusion of the occluded coronary artery is the most immediate and effective treatment. However, therapeutic targeting to promote the repair process has potential for meaningful improvement in clinical outcomes by limiting adverse remodeling and preserving function of the remaining myocardium.

A robust inflammatory response and inefficient repair are driving forces of remodeling and heart failure.[4–7, 72] However, to date, the ability to manipulate this response therapeutically has proven challenging. Indeed, optimal repair requires a delicate balance of tissue destruction and scar formation, neovascularization and wound healing. In this study, we have uncovered an important role for the cytosolic DNA sensing pathway cGAS-STING during myocardial repair after ischemic injury.

Macrophage differentiation and myocardial repair after ischemic injury

Depending on the context, macrophages can promote either inflammation and progression of tissue injury or improve wound healing and tissue remodeling.[1] This duality of function derives from the unique ability of macrophages to exist in a continuum of activation states. The crucial role of monocyte/macrophage transformation from inflammatory to reparative phenotype in post-MI repair has been demonstrated recently.[14] Mice harboring macrophages with impaired ability to transform into reparative macrophages (secondary to deletion of the Trb1 kinase) manifest a dramatic increase in mortality and ventricular rupture after MI when compared to *WT* animals.[14] Here, we report that infarcted hearts in mice lacking *cGAS* manifest no obvious declines in total macrophage infiltration but yet harbor decreased numbers of pro-inflammatory (M1-like) macrophages with a shift toward CD206-positive, reparative (M2-like) cells. Importantly, this shift in monocyte/macrophage pools results in a dramatic decrease in post-MI cardiac rupture and associated mortality.

Changes in the microenvironment that dictate macrophage transformation are poorly understood. Findings reported here point to cytosolic DNA sensing by the cGAS pathway as an important and previously unrecognized driver of the expression of inflammatory macrophage phenotypes. Indeed, cytosolic DNA induced iNOS and CXCL10, key features of inflammatory macrophages, in a cGAS-dependent manner in BMDM. Remarkably, we found the ischemia-induced expression of *CXCL10* depended entirely on an intact cGAS pathway. Our findings are consistent with a model in which biasing macrophages toward the reparative subtype by inactivation of the cGAS-STING pathway promotes myocardial tissue repair (Figure 8).

We report that without cGAS-mediated signaling, macrophages derived from both BMDM and human THP1 monocytes express lower levels of M1 markers, such as CXCL10, and higher levels of markers of the M2 subtype, such as CD163 and fibronectin (Figures 3, S1).[48] However, these cells can still be biased toward the M1 phenotype when exposed to stimulators of the microbial inflammatory response such as LPS. In our *in vivo* model of MI, loss of cGAS promotes accumulation of macrophages strongly positive for CD206 (M2 marker) within the infarct area. As the functional transformation of macrophages (toward or away from M1 or M2) involves hundreds of genes[39], loss of *cGAS* and the ensuing dampened IRF3 response are likely upstream triggers that orchestrate a complex cascade of events. In fact, our findings that *cGAS* downstream targets are among the most down-regulated genes observed in M2 macrophages[39] support a model in which cGAS-mediated cytosolic DNA sensing is crucial in influencing macrophage phenotype during myocardial repair after ischemia injury. However, it is important to emphasize that the M1/M2 dichotomy classification is a useful over-simplification of a broad functional spectrum, one in which M1 and M2 macrophages occupy the opposite extremes and yet a functional continuum exists in between.

Whereas we observed meaningful changes in macrophage behavior, overall inflammatory cytokine levels were not altered significantly in the infarcted cGAS-null heart when compared to the WT. However, specific ISGs such as *Cxcl10*, *IRF7, IFIT1, and IFIT3*, are expressed in ischemic hearts in a cGAS-dependent manner. Indeed, ISG expression is reduced in macrophages treated with IL4 or TGFβ. These anti-inflammatory cytokines,

which can polarize macrophages to the M2-like subtype, have been shown to play important roles in tissue repair remodeling after infarction.

Perhaps the most direct impact on myocardial wound repair of the shift in macrophage phenotype stemming from loss of cGAS is the greater amount of fibronectin produced. Fibronectin is a major component of the provisional matrix after MI to which fibroblasts migrate and proliferate and where they differentiate into myofibroblasts.[73] Thus, fibronectin expression is pivotal in myocardial wound healing. Indeed, our analysis of the MI repair response is consistent with enhanced repair in *cGAS*$^{-/-}$ hearts.

Myocardial infarction is often marked by infarct expansion, disproportionate thinning and dilatation of the infarct segment, which confers meaningful clinical consequences.[72] Infarct expansion gives rise to additional LV dilatation and consequent enhanced stress to remote functioning myocardium. Not surprisingly, patients with expansion of an infarct have diminished exercise tolerance, more heart failure symptoms, and greater early and late mortality than those without expansion.[72] Adequate myofibroblast density limits infarct expansion by promoting deposition of strong and flexible replacement tissue.[74] Indeed, numerous lines of evidence point to malformed scar and high incidence of cardiac rupture when there are defects in fibroblast adhesion, recruitment, and transformation.[75] We show here that inactivation of cGAS promotes M2-like macrophage transformation, deposition of fibronectin, diminished LV dilatation and suppressed infarct expansion. The reparative granular tissue in *cGAS*$^{-/-}$ mice harbors a greater number of myofibroblasts, which contribute to greater collagen density and cross-linked collagen fibrils, which together afford more tensile strength to the tissue. The ultimate consequence is decreased risk of ventricular rupture and improved survival despite absence of change in the size of the original infarct.

We also observe enhanced angiogenesis post-MI in cGAS-null hearts. As new blood vessel formation provides nutrients and supports the provisional matrix and peri-infarct area, effective angiogenesis leads to enhanced myocardial perfusion, reduction in infarct size, and enhanced survival.[76]

cGAS-mediated signaling and the inflammatory response after myocardial infarction

A prior study suggested a role for cGAS in constitutive production of basal levels of IFNs and ISGs[26] in macrophages through tonic signaling[77], which may help to explain the fundamental differences in phenotypes between *WT* and *cGAS*$^{-/-}$ cells at baseline and after DNA stimulation. The *cGAS*$^{-/-}$ macrophage has a signature profile more consistent with that of M2 macrophages, although they cannot be strictly defined as M2 macrophages, a nomenclature assigned to cells after they are stimulated with anti-inflammatory cytokines, such as IL4 and IL13.[53] Moreover, unlike our *in vivo* findings which showed that loss of *cGAS* did not influence the major inflammatory cytokines at the transcript level, *cGAS* loss-of-function in THP1 cells resulted in higher levels of IL1β at baseline and after DNA stimulation (data not shown), highlighting the complexity of macrophage polarization. M1 and M2 macrophages are known to generate (at least) comparable levels of inflammatory cytokines in the heart after myocardial infarction.[37]

Importantly, the beneficial impact of cGAS inactivation does not derive from alterations in major elements of the inflammatory cytokine system, including *IL1β, IL18, IL6,* and *TNFα*, suggesting that myocardial repair can be fostered without interference with pathways mediated by these cytokines. A robust inflammatory response after MI is essential to remove damaged myocardium. However, prolonged and robust inflammation is associated with worse outcomes.[5–7] Although pro-inflammatory cytokines are known to promote tissue destruction and are thought to be responsible for a negative impact on wound healing, they are also profoundly pleiotropic.[78] This pleiotropy is a difficult obstacle to overcome when the aim is to neutralize, antagonize, and block the cytokines.[79] Among many examples, studies have shown that sustained expression of TNFα contributes to the development of heart failure; however, TNFα can also exert cytoprotective effects in a desmin-deficient heart failure model in mice.[80] Moreover, loss of signaling in mice depleted of IL1R1, the only signaling receptor for IL1, not only attenuated the recruitment of inflammatory monocytes/macrophages but diminished recruitment of the reparative macrophage subtype as well.[33] Our results indicate that targeting cGAS may achieve better outcomes without perturbing the intricate and pleiotropic cytokine system. It is also important to emphasize that we examined these cytokines at the level of transcript only, additional studies are necessary to determine the involvement of these important inflammatory pathways.

DNA as a danger signal in myocardial infarction

DNA is normally sequestered within the nucleus and mitochondria, away from the cytosol. cGAS, a recently discovered mechanism of the innate immune response, is the predominant sensor of double-stranded DNA in the cytosol.[18, 19] cGAS recognizes the sugar-phosphate backbone in DNA, and hence the binding between DNA and cGAS is non-specific. TLR9 is also known to recognize DNA inside the cell. However, it is located within the endosome with its binding domain facing the lumen.[45] TLR9 preferentially binds DNA harboring unmethylated CpG motifs prevalent in microbial DNA but much less common in vertebrate genomic DNA.[81] TLR9 has been suggested to mediate the inflammatory response in a heart failure model generated from pressure overload by recognizing mitochondrial DNA.[82] However, increased incidence of cardiac rupture after myocardial infarction in TLR9-null mice was observed with no impact on remodeling and cardiac function.[83] Also, the overall inflammatory responses were comparable between *WT* and *TLR9-null* mice after MI.[83] It is intriguing that loss of DNA sensing in the cytosol (cGAS inactivation) and loss of CpG DNA recognition inside the endosome (TLR9 inactivation) lead to opposite results in terms of maintenance of cardiac tissue integrity. However, we suggest that cGAS-specific effects on macrophage transformation may hold the key.[83, 84] Unlike cGAS, TLR9-mediated signaling is unable to activate IRF3[85], which is a crucial point in sustaining pro-inflammatory macrophages.[86] Also, differences in the primary cell types in which each specific pathway operates may contribute. Indeed, some evidence suggests that fibroblasts are the primary cell type affected by TLR9 signaling.[83, 84]

Future directions and perspective

Our findings raise a number of intriguing questions. First, the current standard of care for patients with acute coronary occlusion is reperfusion therapy; hence, determining the impact of cGAS-STING in a model of ischemia/reperfusion injury will be of interest. Whereas

reperfusion blunts injury and infarct size, it also evokes damage of its own that contributes to final infarct injury, and it will be intriguing to evaluate this pathway in that context. Second, evidence suggests that inflammation is a prominent feature in the chronic remodeling phase after MI[87], and elucidation of this pathway in this phase of the process will be informative. Third, it is known that cardiac-resident macrophages and those derived from peripheral circulating monocytes have different functions.[58] Delineation of the contributions of distinct groups of macrophages will help to differentiate the impact of cGAS in maintaining homeostasis and following stress. Finally, while it is clear that silencing cGAS in the entire organism is protective in MI, whether the phenotype derives exclusively from monocyte/macrophage-specific cGAS function is unknown, as activation of the pathway in other cell types might conceivably contribute to the overall benefit.

In summary, this report identifies cytosolic DNA sensing mediated by cGAS as a novel pattern recognition receptor in myocardial ischemic injury and unveils its important role in governing macrophage function during repair of the damaged heart. Inhibition of this pathway protects the heart by improving early survival, inhibiting pathological remodeling, promoting angiogenesis, and preserving cardiac function. The underlying mechanism is that loss of cGAS improves the repair process by priming macrophages toward a reparative phenotype. Further, our findings provide insight into the microenvironmental cues and mechanisms controlling the transition of pro-inflammatory macrophages to a reparative subtype and could serve as potential targets for future novel interventions aimed at macrophage transformation.

Supplementary Material

Refer to Web version on PubMed Central for supplementary material.

Acknowledgments

We thank Drs. Zhiping Liu and Anwarul Ferdous for valuable suggestions, Dr. Xiang Lou for isolating adult cardiomyocytes, Dr. Wei Tan for performing some of the MI surgeries, and Fenghe Du for critical support.

SOURCES OF FUNDING

This work was supported by grants from the National Institutes of Health (K08 HL116801 to DC; HL-120732 to JAH; HL-126012 to JAH; HL-128215 to JAH), American Heart Association (14SFRN20510023 to JAH; 14SFRN20670003 to JAH), Fondation Leducq (11CVD04, to JAH), and Cancer Prevention and Research Institute of Texas (RP110486P3, to JAH).

References

1. Nahrendorf M, Pittet MJ, Swirski FK. Monocytes: protagonists of infarct inflammation and repair after myocardial infarction. Circulation. 2010; 121:2437–2445. [PubMed: 20530020]
2. Mann DL. Innate immunity and the failing heart: the cytokine hypothesis revisited. Circ Res. 2015; 116:1254–1268. [PubMed: 25814686]
3. Prabhu SD, Frangogiannis NG. The Biological Basis for Cardiac Repair After Myocardial Infarction: From Inflammation to Fibrosis. Circ Res. 2016; 119:91–112. [PubMed: 27340270]
4. Sager HB, Heidt T, Hulsmans M, Dutta P, Courties G, Sebas M, Wojtkiewicz GR, Tricot B, Iwamoto Y, Sun Y, Weissleder R, Libby P, Swirski FK, Nahrendorf M. Targeting Interleukin-1beta Reduces Leukocyte Production After Acute Myocardial Infarction. Circulation. 2015; 132:1880–1890. [PubMed: 26358260]

5. Aoki S, Nakagomi A, Asai K, Takano H, Yasutake M, Seino Y, Mizuno K. Elevated peripheral blood mononuclear cell count is an independent predictor of left ventricular remodeling in patients with acute myocardial infarction. J Cardiol. 2011; 57:202–207. [PubMed: 21168993]
6. Shimpo M, Morrow DA, Weinberg EO, Sabatine MS, Murphy SA, Antman EM, Lee RT. Serum levels of the interleukin-1 receptor family member ST2 predict mortality and clinical outcome in acute myocardial infarction. Circulation. 2004; 109:2186–190. [PubMed: 15117853]
7. Suleiman M, Khatib R, Agmon Y, Mahamid R, Boulos M, Kapeliovich M, Levy Y, Beyar R, Markiewicz W, Hammerman H, Aronson D. Early inflammation and risk of long-term development of heart failure and mortality in survivors of acute myocardial infarction predictive role of C-reactive protein. J Am Coll Cardiol. 2006; 47:962–968. [PubMed: 16516078]
8. van Hout GP, Jansen of Lorkeers SJ, Wever KE, Sena ES, Kouwenberg LH, van Solinge WW, Macleod MR, Doevendans PA, Pasterkamp G, Chamuleau SA, Hoefer IE. Translational failure of anti-inflammatory compounds for myocardial infarction: a meta-analysis of large animal models. Cardiovas Res. 2016; 109:240–248.
9. Seropian IM, Toldo S, Van Tassell BW, Abbate A. Anti-inflammatory strategies for ventricular remodeling following ST-segment elevation acute myocardial infarction. J Am Coll Cardiol. 2014; 63:1593–1603. [PubMed: 24530674]
10. Nahrendorf M, Swirski FK, Aikawa E, Stangenberg L, Wurdinger T, Figueiredo JL, Libby P, Weissleder R, Pittet MJ. The healing myocardium sequentially mobilizes two monocyte subsets with divergent and complementary functions. J Expl Med. 2007; 204:3037–3047.
11. Panizzi P, Swirski FK, Figueiredo JL, Waterman P, Sosnovik DE, Aikawa E, Libby P, Pittet M, Weissleder R, Nahrendorf M. Impaired infarct healing in atherosclerotic mice with Ly-6C(hi) monocytosis. J Am Coll Cardiol. 2010; 55:1629–1638. [PubMed: 20378083]
12. Troidl C, Mollmann H, Nef H, Masseli F, Voss S, Szardien S, Willmer M, Rolf A, Rixe J, Troidl K, Kostin S, Hamm C, Elsasser A. Classically and alternatively activated macrophages contribute to tissue remodelling after myocardial infarction. J cell mol med. 2009; 13:3485–3496. [PubMed: 19228260]
13. Hilgendorf I, Gerhardt LM, Tan TC, Winter C, Holderried TA, Chousterman BG, Iwamoto Y, Liao R, Zirlik A, Scherer-Crosbie M, Hedrick CC, Libby P, Nahrendorf M, Weissleder R, Swirski FK. Ly-6Chigh monocytes depend on Nr4a1 to balance both inflammatory and reparative phases in the infarcted myocardium. Circ Res. 2014; 114:1611–1622. [PubMed: 24625784]
14. Shiraishi M, Shintani Y, Shintani Y, Ishida H, Saba R, Yamaguchi A, Adachi H, Yashiro K, Suzuki K. Alternatively activated macrophages determine repair of the infarcted adult murine heart. J clin invest. 2016; 126:2151–2166. [PubMed: 27140396]
15. Swirski FK, Nahrendorf M, Etzrodt M, Wildgruber M, Cortez-Retamozo V, Panizzi P, Figueiredo JL, Kohler RH, Chudnovskiy A, Waterman P, Aikawa E, Mempel TR, Libby P, Weissleder R, Pittet MJ. Identification of splenic reservoir monocytes and their deployment to inflammatory sites. Science. 2009; 325:612–616. [PubMed: 19644120]
16. Emami H, Singh P, MacNabb M, Vucic E, Lavender Z, Rudd JH, Fayad ZA, Lehrer-Graiwer J, Korsgren M, Figueroa AL, Fredrickson J, Rubin B, Hoffmann U, Truong QA, Min JK, Baruch A, Nasir K, Nahrendorf M, Tawakol A. Splenic metabolic activity predicts risk of future cardiovascular events: demonstration of a cardiosplenic axis in humans. JACC Cardiovascular imaging. 2015; 8:121–130. [PubMed: 25577441]
17. Schaefer L. Complexity of danger: the diverse nature of damage-associated molecular patterns. J biol chem. 2014; 289:35237–35245. [PubMed: 25391648]
18. Sun L, Wu J, Du F, Chen X, Chen ZJ. Cyclic GMP-AMP synthase is a cytosolic DNA sensor that activates the type I interferon pathway. Science. 2013; 339:786–791. [PubMed: 23258413]
19. Li XD, Wu J, Gao D, Wang H, Sun L, Chen ZJ. Pivotal roles of cGAS-cGAMP signaling in antiviral defense and immune adjuvant effects. Science. 2013; 341:1390–1394. [PubMed: 23989956]
20. Wassermann R, Gulen MF, Sala C, Perin SG, Lou Y, Rybniker J, Schmid-Burgk JL, Schmidt T, Hornung V, Cole ST, Ablasser A. Mycobacterium tuberculosis Differentially Activates cGAS- and Inflammasome-Dependent Intracellular Immune Responses through ESX-1. Cell host & microbe. 2015; 17:799–810. [PubMed: 26048138]

21. Paijo J, Doring M, Spanier J, Grabski E, Nooruzzaman M, Schmidt T, Witte G, Messerle M, Hornung V, Kaever V, Kalinke U. cGAS Senses Human Cytomegalovirus and Induces Type I Interferon Responses in Human Monocyte-Derived Cells. PLoS pathogens. 2016; 12:e1005546. [PubMed: 27058035]
22. Chen Q, Sun L, Chen ZJ. Regulation and function of the cGAS-STING pathway of cytosolic DNA sensing. Nat immunol. 2016; 17:1142–1149. [PubMed: 27648547]
23. Glass CK, Natoli G. Molecular control of activation and priming in macrophages. Nat immunol. 2016; 17:26–33. [PubMed: 26681459]
24. Carty M, Reinert L, Paludan SR, Bowie AG. Innate antiviral signalling in the central nervous system. Trends immunol. 2014; 35:79–87. [PubMed: 24316012]
25. Gao D, Li T, Li XD, Chen X, Li QZ, Wight-Carter M, Chen ZJ. Activation of cyclic GMP-AMP synthase by self-DNA causes autoimmune diseases. Proc Nat Acad Sci USA. 2015; 112:E5699–E5705. [PubMed: 26371324]
26. Schoggins JW, MacDuff DA, Imanaka N, Gainey MD, Shrestha B, Eitson JL, Mar KB, Richardson RB, Ratushny AV, Litvak V, Dabelic R, Manicassamy B, Aitchison JD, Aderem A, Elliott RM, Garcia-Sastre A, Racaniello V, Snijder EJ, Yokoyama WM, Diamond MS, Virgin HW, Rice CM. Pan-viral specificity of IFN-induced genes reveals new roles for cGAS in innate immunity. Nature. 2014; 505:691–695. [PubMed: 24284630]
27. West AP, Khoury-Hanold W, Staron M, Tal MC, Pineda CM, Lang SM, Bestwick M, Duguay BA, Raimundo N, MacDuff DA, Kaech SM, Smiley JR, Means RE, Iwasaki A, Shadel GS. Mitochondrial DNA stress primes the antiviral innate immune response. Nature. 2015; 520:553–557. [PubMed: 25642965]
28. Gentili M, Kowal J, Tkach M, Satoh T, Lahaye X, Conrad C, Boyron M, Lombard B, Durand S, Kroemer G, Loew D, Dalod M, Thery C, Manel N. Transmission of innate immune signaling by packaging of cGAMP in viral particles. Science. 2015; 349:1232–1236. [PubMed: 26229115]
29. Bae YS, Lee JH, Choi SH, Kim S, Almazan F, Witztum JL, Miller YI. Macrophages generate reactive oxygen species in response to minimally oxidized low-density lipoprotein: toll-like receptor 4- and spleen tyrosine kinase-dependent activation of NADPH oxidase 2. Circulation research. 2009; 104:210–8. 21p–218. [PubMed: 19096031]
30. Moore KJ, Sheedy FJ, Fisher EA. Macrophages in atherosclerosis: a dynamic balance. Nat rev Immunol. 2013; 13:709–721. [PubMed: 23995626]
31. Hermansson C, Lundqvist A, Magnusson LU, Ullstrom C, Bergstrom G, Hulten LM. Macrophage CD14 expression in human carotid plaques is associated with complicated lesions, correlates with thrombosis, and is reduced by angiotensin receptor blocker treatment. Internat immunopharmacol. 2014; 22:318–323.
32. Bujak M, Dobaczewski M, Chatila K, Mendoza LH, Li N, Reddy A, Frangogiannis NG. Interleukin-1 receptor type I signaling critically regulates infarct healing and cardiac remodeling. Am j pathol. 2008; 173:57–67. [PubMed: 18535174]
33. Saxena A, Chen W, Su Y, Rai V, Uche OU, Li N, Frangogiannis NG. IL-1 induces proinflammatory leukocyte infiltration and regulates fibroblast phenotype in the infarcted myocardium. J immunol. 2013; 191:4838–4848. [PubMed: 24078695]
34. Ridker PM, Everett BM, Thuren T, MacFadyen JG, Chang WH, Ballantyne C, Fonseca F, Nicolau J, Koenig W, Anker SD, Kastelein JJP, Cornel JH, Pais P, Pella D, Genest J, Cifkova R, Lorenzatti A, Forster T, Kobalava Z, Vida-Simiti L, Flather M, Shimokawa H, Ogawa H, Dellborg M, Rossi PRF, Troquay RPT, Libby P, Glynn RJ, Group CT. Antiinflammatory Therapy with Canakinumab for Atherosclerotic Disease. New Eng J med. 2017; 377:1119–1131. [PubMed: 28845751]
35. Abbate A, Van Tassell BW, Biondi-Zoccai G, Kontos MC, Grizzard JD, Spillman DW, Oddi C, Roberts CS, Melchior RD, Mueller GH, Abouzaki NA, Rengel LR, Varma A, Gambill ML, Falcao RA, Voelkel NF, Dinarello CA, Vetrovec GW. Effects of interleukin-1 blockade with anakinra on adverse cardiac remodeling and heart failure after acute myocardial infarction [from the Virginia Commonwealth University-Anakinra Remodeling Trial (2) (VCU-ART2) pilot study]. Am J cardiol. 2013; 111:1394–1400. [PubMed: 23453459]
36. Hwang MW, Matsumori A, Furukawa Y, Ono K, Okada M, Iwasaki A, Hara M, Miyamoto T, Touma M, Sasayama S. Neutralization of interleukin-1beta in the acute phase of myocardial

infarction promotes the progression of left ventricular remodeling. J Am Coll Cardiol. 2001; 38:1546–1553. [PubMed: 11691538]

37. Yan X, Anzai A, Katsumata Y, Matsuhashi T, Ito K, Endo J, Yamamoto T, Takeshima A, Shinmura K, Shen W, Fukuda K, Sano M. Temporal dynamics of cardiac immune cell accumulation following acute myocardial infarction. J mol cell cardiol. 2013; 62:24–35. [PubMed: 23644221]
38. Lawrence T, Natoli G. Transcriptional regulation of macrophage polarization: enabling diversity with identity. Nat rev iImmunol. 2011; 11:750–761.
39. Jablonski KA, Amici SA, Webb LM, de Ruiz-Rosado JD, Popovich PG, Partida-Sanchez S, Guerau-de-Arellano M. Novel Markers to Delineate Murine M1 and M2 Macrophages. PloS one. 2015; 10:e0145342. [PubMed: 26699615]
40. Kenneth Mallory G, White PD, Salcedo-Salgar J. The speed of healing of myocardial infarction. Am Heart J. 18:647–671.
41. Kovacevic Z, Sahni S, Lok H, Davies MJ, Wink DA, Richardson DR. Regulation and control of nitric oxide (NO) in macrophages: Protecting the “professional killer cell” from its own cytotoxic arsenal via MRP1 and GSTP1. Biochim Biophys Acta. 2017; 1861:995–999. [PubMed: 28219722]
42. Rodriguez PC, Ochoa AC, Al-Khami AA. Arginine Metabolism in Myeloid Cells Shapes Innate and Adaptive Immunity. Front immunol. 2017; 8:93. [PubMed: 28223985]
43. Gordon S. Alternative activation of macrophages. Nat rev Immunol. 2003; 3:23–35. [PubMed: 12511873]
44. Morris SM Jr, Kepka-Lenhart D, Chen LC. Differential regulation of arginases and inducible nitric oxide synthase in murine macrophage cells. Am J Physiol. 1998; 275:E740–E747. [PubMed: 9814991]
45. Cai X, Chiu Y-H, Chen ZJ. The cGAS-cGAMP-STING pathway of cytosolic DNA sensing and signaling. Mol Cell. 2014; 54:289–296. [PubMed: 24766893]
46. Mia S, Warnecke A, Zhang XM, Malmstrom V, Harris RA. An optimized Protocol for Human M2 Macrophages using M-CSF and IL-4/IL-10/TGF-beta Yields a Dominant Immunosuppressive Phenotype. Scand J Immunol. 2014; 79:305–314. [PubMed: 24521472]
47. Bujak M, Frangogiannis NG. The role of TGF-beta signaling in myocardial infarction and cardiac remodeling. Cardiovasc Res. 2007; 74:184–195. [PubMed: 17109837]
48. Genin M, Clement F, Fattaccioli A, Raes M, Michiels C. M1 and M2 macrophages derived from THP-1 cells differentially modulate the response of cancer cells to etoposide. BMC cancer. 2015; 15:577. [PubMed: 26253167]
49. Castro SA, Collighan R, Lambert PA, Dias IH, Chauhan P, Bland CE, Milic I, Milward MR, Cooper PR, Devitt A. Porphyromonas gingivalis gingipains cause defective macrophage migration towards apoptotic cells and inhibit phagocytosis of primary apoptotic neutrophils. Cell death dis. 2017; 8:e2644. [PubMed: 28252646]
50. Ward LJ, Ljunggren SA, Karlsson H, Li W, Yuan X-M. Exposure to atheroma-relevant 7-oxysterols causes proteomic alterations in cell death, cellular longevity, and lipid metabolism in THP-1 macrophages. PloS one. 2017; 12:e0174475. [PubMed: 28350877]
51. Kou JY, Li Y, Zhong ZY, Jiang YQ, Li XS, Han XB, Liu ZN, Tian Y, Yang LM. Berberine-sonodynamic therapy induces autophagy and lipid unloading in macrophage. Cell death dis. 2017; 8:e2558. [PubMed: 28102849]
52. Mantovani A, Sica A, Sozzani S, Allavena P, Vecchi A, Locati M. The chemokine system in diverse forms of macrophage activation and polarization. Trend immunol. 2004; 25:677–686.
53. Murray PJ, Allen JE, Biswas SK, Fisher EA, Gilroy DW, Goerdt S, Gordon S, Hamilton JA, Ivashkiv LB, Lawrence T, Locati M, Mantovani A, Martinez FO, Mege JL, Mosser DM, Natoli G, Saeij JP, Schultze JL, Shirey KA, Sica A, Suttles J, Udalova I, van Ginderachter JA, Vogel SN, Wynn TA. Macrophage activation and polarization: nomenclature and experimental guidelines. Immunity. 2014; 41:14–20. [PubMed: 25035950]
54. Willems IE, Arends JW, Daemen MJ. Tenascin and fibronectin expression in healing human myocardial scars. J Pathol. 1996; 179:321–325. [PubMed: 8774490]
55. Casscells W, Kimura H, Sanchez JA, Yu ZX, Ferrans VJ. Immunohistochemical study of fibronectin in experimental myocardial infarction. Am J pathol. 1990; 137:801–810. [PubMed: 2221013]

56. Serini G, Bochaton-Piallat ML, Ropraz P, Geinoz A, Borsi L, Zardi L, Gabbiani G. The fibronectin domain ED-A is crucial for myofibroblastic phenotype induction by transforming growth factor-beta1. J Cell Biol. 1998; 142:873–881. [PubMed: 9700173]
57. Virag JI, Murry CE. Myofibroblast and endothelial cell proliferation during murine myocardial infarct repair. Am j pathol. 2003; 163:2433–2440. [PubMed: 14633615]
58. Epelman S, Lavine KJ, Beaudin AE, Sojka DK, Carrero JA, Calderon B, Brija T, Gautier EL, Ivanov S, Satpathy AT, Schilling JD, Schwendener R, Sergin I, Razani B, Forsberg EC, Yokoyama WM, Unanue ER, Colonna M, Randolph GJ, Mann DL. Embryonic and adult-derived resident cardiac macrophages are maintained through distinct mechanisms at steady state and during inflammation. Immunity. 2014; 40:91–104. [PubMed: 24439267]
59. Leblond AL, Klinkert K, Martin K, Turner EC, Kumar AH, Browne T, Caplice NM. Systemic and Cardiac Depletion of M2 Macrophage through CSF-1R Signaling Inhibition Alters Cardiac Function Post Myocardial Infarction. PloS one. 2015; 10:e0137515. [PubMed: 26407006]
60. Wynn TA, Ramalingam TR. Mechanisms of fibrosis: therapeutic translation for fibrotic disease. Nat med. 2012; 18:1028–1040. [PubMed: 22772564]
61. Shinde AV, Humeres C, Frangogiannis NG. The role of alpha-smooth muscle actin in fibroblast-mediated matrix contraction and remodeling. Biochim Biophys Acta. 2017; 1863:298–309. [PubMed: 27825850]
62. Mantovani A, Marchesi F, Malesci A, Laghi L, Allavena P. Tumour-associated macrophages as treatment targets in oncology. Nat Rev Clin Oncol. 2017; 14:399–416. [PubMed: 28117416]
63. Zajac E, Schweighofer B, Kupriyanova TA, Juncker-Jensen A, Minder P, Quigley JP, Deryugina EI. Angiogenic capacity of M1- and M2-polarized macrophages is determined by the levels of TIMP-1 complexed with their secreted proMMP-9. Blood. 2013; 122:4054–4067. [PubMed: 24174628]
64. Takagawa J, Zhang Y, Wong ML, Sievers RE, Kapasi NK, Wang Y, Yeghiazarians Y, Lee RJ, Grossman W, Springer ML. Myocardial infarct size measurement in the mouse chronic infarction model: comparison of area- and length-based approaches. J appl physiol. 2007; 102:2104–2111. [PubMed: 17347379]
65. Chan W, Duffy SJ, White DA, Gao XM, Du XJ, Ellims AH, Dart AM, Taylor AJ. Acute left ventricular remodeling following myocardial infarction: coupling of regional healing with remote extracellular matrix expansion. JACC Cardiovascular imaging. 2012; 5:884–893. [PubMed: 22974800]
66. Lattouf R, Younes R, Lutomski D, Naaman N, Godeau G, Senni K, Changotade S. Picrosirius red staining: a useful tool to appraise collagen networks in normal and pathological tissues. J histochem cytochem. 2014; 62:751–758. [PubMed: 25023614]
67. Horckmans M, Ring L, Duchene J, Santovito D, Schloss MJ, Drechsler M, Weber C, Soehnlein O, Steffens S. Neutrophils orchestrate post-myocardial infarction healing by polarizing macrophages towards a reparative phenotype. Eur Heart J. 2017; 38:187–197. [PubMed: 28158426]
68. Coleman R. Picrosirius red staining revisited. Acta histochemica. 2011; 113:231–233. [PubMed: 20188402]
69. van Amerongen MJ, Harmsen MC, van Rooijen N, Petersen AH, van Luyn MJ. Macrophage depletion impairs wound healing and increases left ventricular remodeling after myocardial injury in mice. Am J pathol. 2007; 170:818–829. [PubMed: 17322368]
70. Gao XM, Xu Q, Kiriazis H, Dart AM, Du XJ. Mouse model of post-infarct ventricular rupture: time course, strain- and gender-dependency, tensile strength, and histopathology. Cardiovasc Res. 2005; 65:469–477. [PubMed: 15639486]
71. Pouleur AC, Barkoudah E, Uno H, Skali H, Finn PV, Zelenkofske SL, Belenkov YN, Mareev V, Velazquez EJ, Rouleau JL, Maggioni AP, Kober L, Califf RM, McMurray JJ, Pfeffer MA, Solomon SD, Investigators V. Pathogenesis of sudden unexpected death in a clinical trial of patients with myocardial infarction and left ventricular dysfunction, heart failure, or both. Circulation. 2010; 122:597–602. [PubMed: 20660803]
72. Weisman HF, Healy B. Myocardial infarct expansion, infarct extension, and reinfarction: pathophysiologic concepts. Prog cardiovasc dis. 1987; 30:73–110. [PubMed: 2888158]

73. Dobaczewski M, de Haan JJ, Frangogiannis NG. The extracellular matrix modulates fibroblast phenotype and function in the infarcted myocardium. J cardiovasc translat res. 2012; 5:837–847.
74. Turner NA, Porter KE. Function and fate of myofibroblasts after myocardial infarction. Fibrogenesis tissue repair. 2013; 6:5. [PubMed: 23448358]
75. van den Borne SW, Diez J, Blankesteijn WM, Verjans J, Hofstra L, Narula J. Myocardial remodeling after infarction: the role of myofibroblasts. Nat rev Cardiol. 2010; 7:30–37. [PubMed: 19949426]
76. Zangi L, Lui KO, von Gise A, Ma Q, Ebina W, Ptaszek LM, Spater D, Xu H, Tabebordbar M, Gorbatov R, Sena B, Nahrendorf M, Briscoe DM, Li RA, Wagers AJ, Rossi DJ, Pu WT, Chien KR. Modified mRNA directs the fate of heart progenitor cells and induces vascular regeneration after myocardial infarction. Nat biotechnol. 2013; 31:898–907. [PubMed: 24013197]
77. Gough DJ, Messina NL, Clarke CJ, Johnstone RW, Levy DE. Constitutive type I interferon modulates homeostatic balance through tonic signaling. Immunity. 2012; 36:166–174. [PubMed: 22365663]
78. Frangogiannis NG. The inflammatory response in myocardial injury, repair, and remodelling. Nat rev Cardiol. 2014; 11:255–265. [PubMed: 24663091]
79. Chung ES, Packer M, Lo KH, Fasanmade AA, Willerson JT. Anti TNFTACHFI. Randomized, double-blind, placebo-controlled, pilot trial of infliximab, a chimeric monoclonal antibody to tumor necrosis factor-alpha, in patients with moderate-to-severe heart failure: results of the anti-TNF Therapy Against Congestive Heart Failure (ATTACH) trial. Circulation. 2003; 107:3133–3140. [PubMed: 12796126]
80. Papathanasiou S, Rickelt S, Soriano ME, Schips TG, Maier HJ, Davos CH, Varela A, Kaklamanis L, Mann DL, Capetanaki Y. Tumor necrosis factor-alpha confers cardioprotection through ectopic expression of keratins K8 and K18. Nat med. 2015; 21:1076–1084. [PubMed: 26280121]
81. Krieg AM, Yi AK, Matson S, Waldschmidt TJ, Bishop GA, Teasdale R, Koretzky GA, Klinman DM. CpG motifs in bacterial DNA trigger direct B-cell activation. Nature. 1995; 374:546–549. [PubMed: 7700380]
82. Oka T, Hikoso S, Yamaguchi O, Taneike M, Takeda T, Tamai T, Oyabu J, Murakawa T, Nakayama H, Nishida K, Akira S, Yamamoto A, Komuro I, Otsu K. Mitochondrial DNA that escapes from autophagy causes inflammation and heart failure. Nature. 2012; 485:251–255. [PubMed: 22535248]
83. Omiya S, Omori Y, Taneike M, Protti A, Yamaguchi O, Akira S, Shah AM, Nishida K, Otsu K. Toll-like receptor 9 prevents cardiac rupture after myocardial infarction in mice independently of inflammation. Am J physiol Heart circ physiol. 2016; 311:H1485–H1497. [PubMed: 27769998]
84. Ohm IK, Alfsnes K, Belland Olsen M, Ranheim T, Sandanger O, Dahl TB, Aukrust P, Finsen AV, Yndestad A, Vinge LE. Toll-like receptor 9 mediated responses in cardiac fibroblasts. PloS one. 2014; 9:e104398. [PubMed: 25126740]
85. Gay NJ, Symmons MF, Gangloff M, Bryant CE. Assembly and localization of Toll-like receptor signalling complexes. Nat rev Immunol. 2014; 14:546–558. [PubMed: 25060580]
86. Bjorkbacka H, Fitzgerald KA, Huet F, Li X, Gregory JA, Lee MA, Ordija CM, Dowley NE, Golenbock DT, Freeman MW. The induction of macrophage gene expression by LPS predominantly utilizes Myd88-independent signaling cascades. Physiol genom. 2004; 19:319–330.
87. Westman PC, Lipinski MJ, Luger D, Waksman R, Bonow RO, Wu E, Epstein SE. Inflammation as a Driver of Adverse Left Ventricular Remodeling After Acute Myocardial Infarction. J Am Coll Cardiol. 2016; 67:2050–2060. [PubMed: 27126533]

Clinical Perspective

What is new?

- We report that release of DNA from necrotic tissue during myocardial infarction triggers in macrophages a recently described innate immune response.
- This response, in turn, promotes an inflammatory macrophage phenotype.
- Suppression of the pathway promotes emergence of reparative macrophages, thereby mitigating pathological ventricular remodeling.

What are the clinical implications?

- These results reveal that a cytosolic DNA receptor functions during cardiac ischemia as a pattern recognition receptor in the sterile immune response.
- As modulators of this pathway are currently in clinical use, our findings raise the prospect of new treatment options to combat ischemic heart disease and its progression to heart failure.

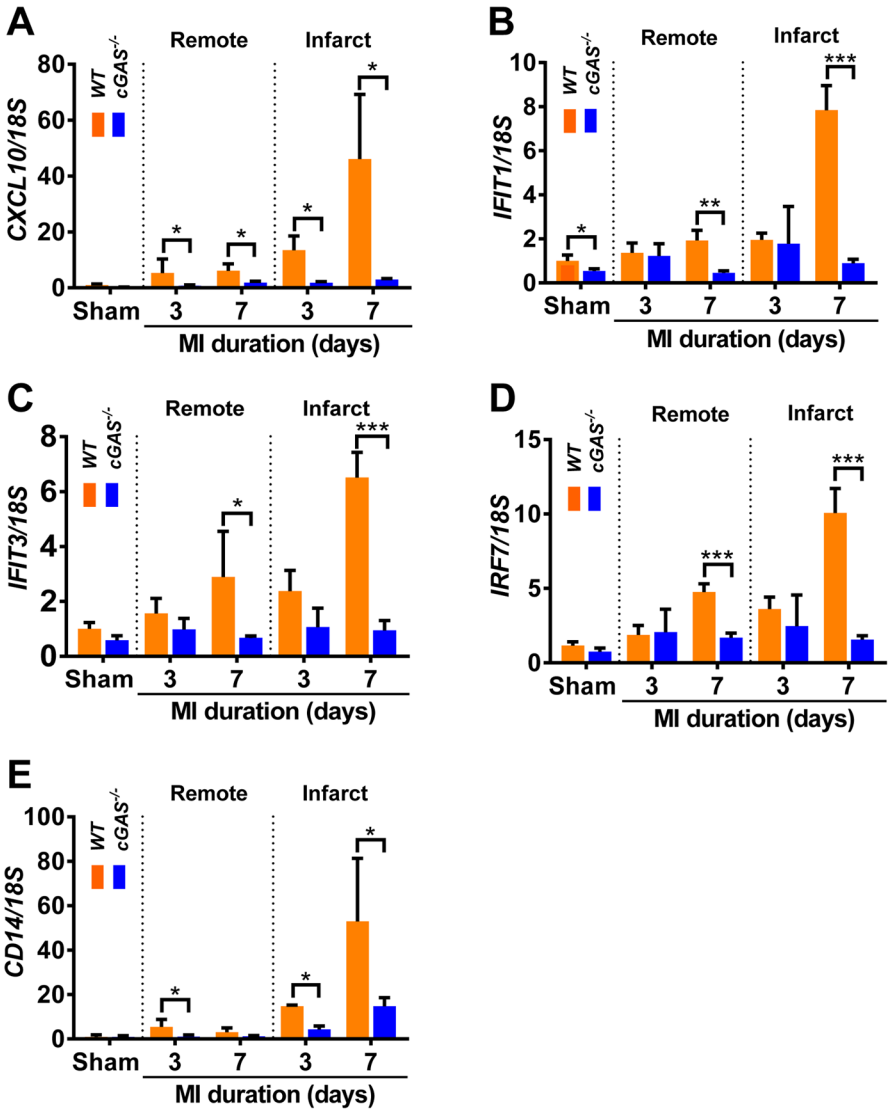

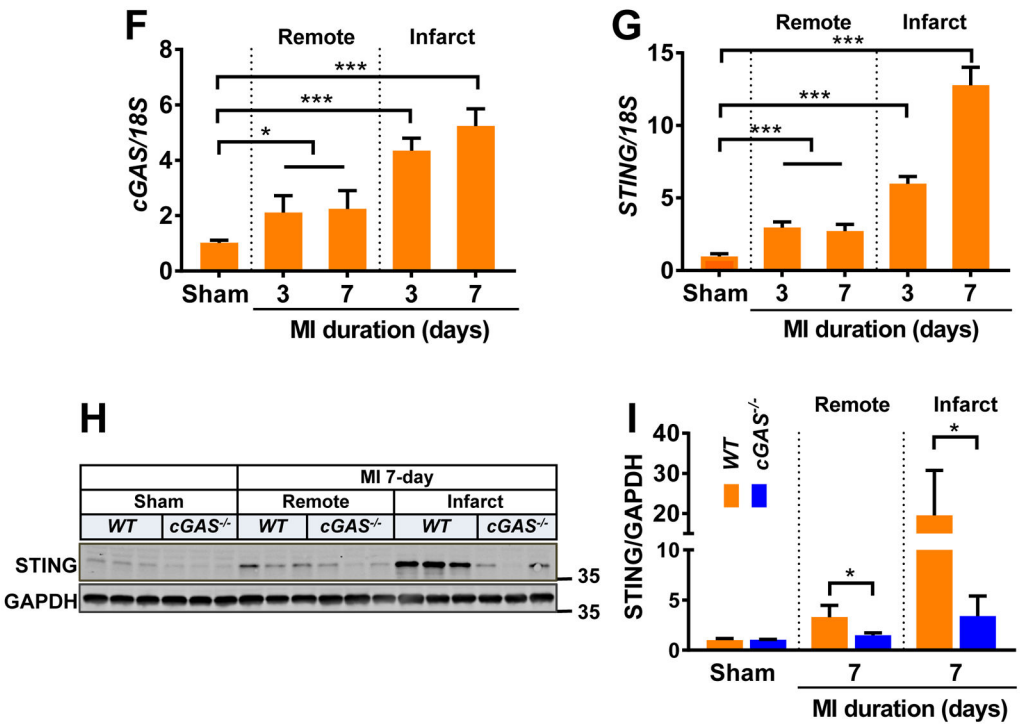

Figure 1. Myocardial ischemia activates cGAS-mediated signaling

Ventricles collected from sham- or MI-operated animals were separated into infarct and remote zones. Quantitative RT-PCR was performed to evaluate transcript abundances of interferon-stimulated genes (ISG) activated by cGAS-STING. ISGs examined included *CXCL10* (**A**), *IFIT1* (**B**), *IFIT3* (**C**), *IRF7* (**D**), and *CD14* (**E**). Infarction elicited significant increases of ISG transcripts exclusively in *WT* animals. **F**. *cGAS* expression in response to infarction in *WT* hearts. **G**. Increases in *STING* transcript in response to infarction in *WT* animals. **H**. Infarction-induced up-regulation of STING protein. **I**. Quantified data depicted in **H**. n=3–7 in infarcted mice; n=3 sham controls. *p<0.05, **p<0.01, **p<0.001.

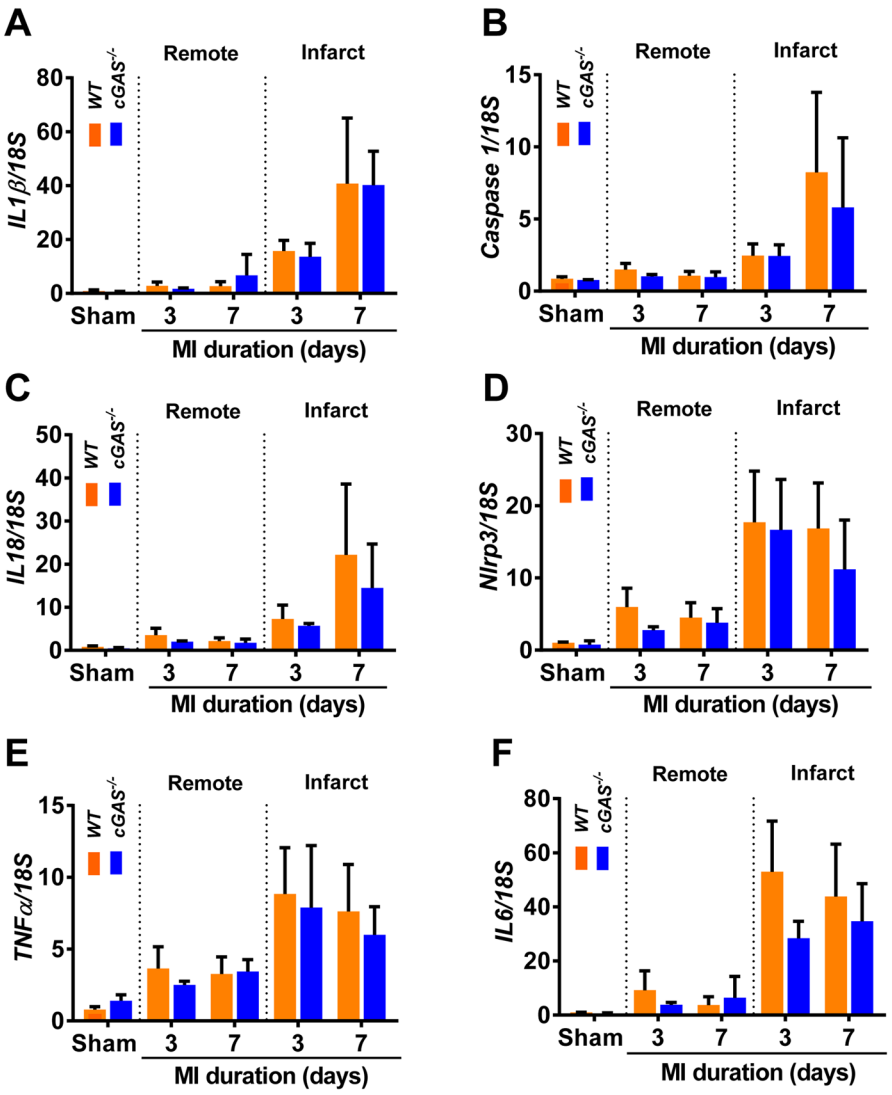

Figure 2. No impact of silencing of cGAS-mediated signaling on the major inflammatory responses after myocardial infarction

WT and *cGAS*$^{-/-}$ mice were subjected to LAD ligation. Three and seven days after surgery, ventricular tissue was collected from infarct and remote areas, and RNA was harvested. Quantitative RT-PCR was performed using primers for *IL1β* (**A**), *caspase 1* (**B**), *IL18* (**C**), *Nlrp3* (**D**), *TNFα* (**E**), and *IL6* (**F**). n=3–7 in infarcted mice; n=3 sham controls.

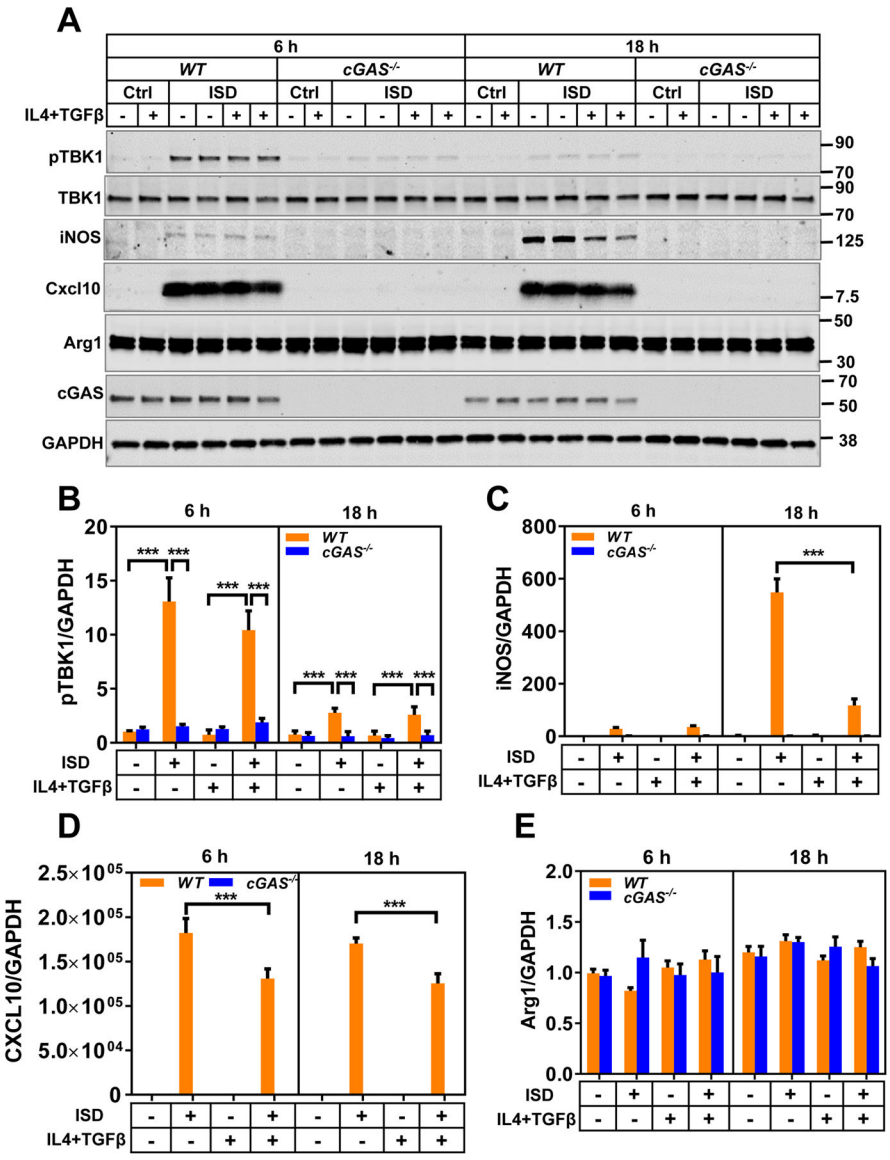

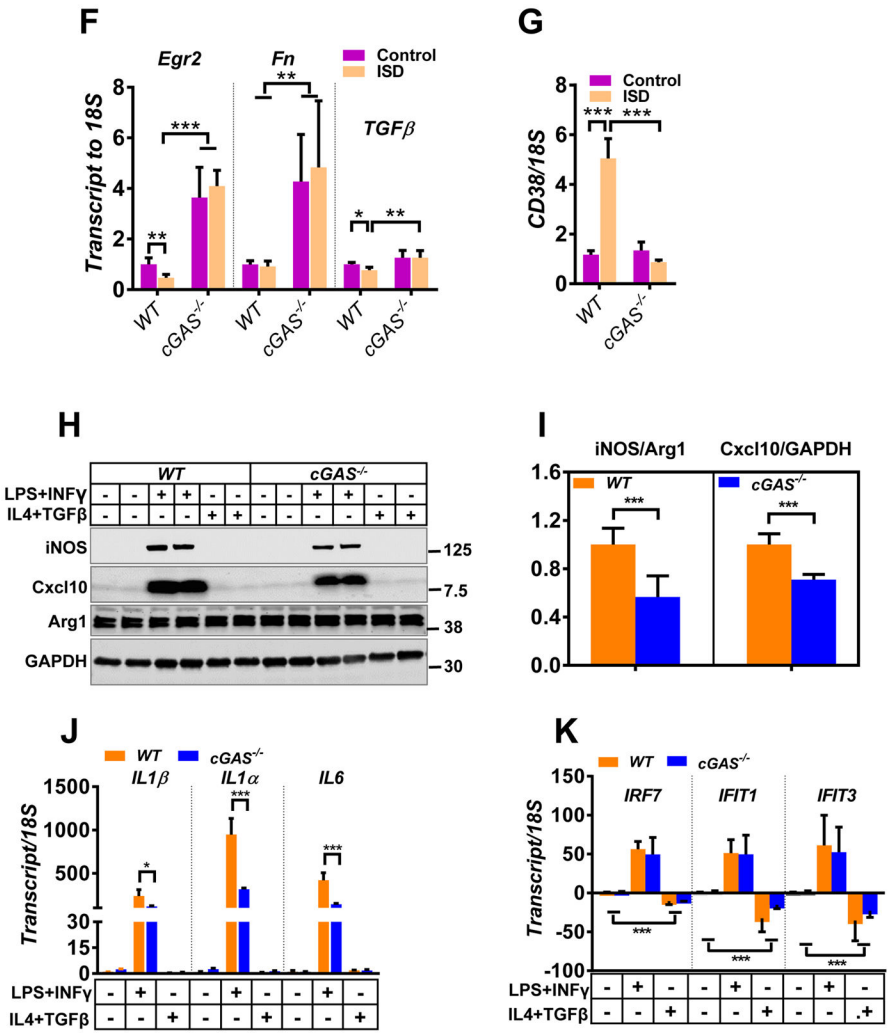

Figure 3. Cytosolic DNA-induced iNOS and CXCl10 expression is cGAS dependent

Macrophages differentiated from bone marrow cells were transfected with ISD for 5 hours. After transfection, the cells were incubated with or without IL4 and TGFβ for an additional 1 hour or 13 hours (total experiment time 6 hours and 18 hours, respectively) before they were harvested for immunoblot analysis. **A.** Time-dependent changes in pTBK1, iNOS, Cxcl10, and Arg1. **B.** Quantification of pTBK1. **C.** Summarized data for iNOS protein induction. **D.** Aggregated results for Cxcl10. **E.** Summarized data for Arg1. **F and G.** The expression of *Egr2, Fn, TGFβ*, and *CD38* in *WT* and *cGAS*$^{-/-}$ macrophages at baseline or after ISD stimulation for 18 hours. **H.** BMDM were stimulated with polarizing agents that promote M1 (LPS and IFNγ) or M2 (IL4 and TGFβ) phenotypes for 24 h. Induction of iNOS and Cxcl10 were examined. **I.** Ratio of iNOS to Arg1 and levels of Cxcl10 after treatment with LPS and IFNγ. **J.** The expression of *IL1β, IL1α,* and *IL6* induced by LPS and IFNγ in *WT* and *cGAS*$^{-/-}$ macrophages. **K.** The response of *IRF7, IFIT1*, and *IFIT3* to M1 and M2 polarizing agents in *WT* and *cGAS*$^{-/-}$ BMDM. n=3–5. *p<0.05, **p<0.01, **p<0.001.

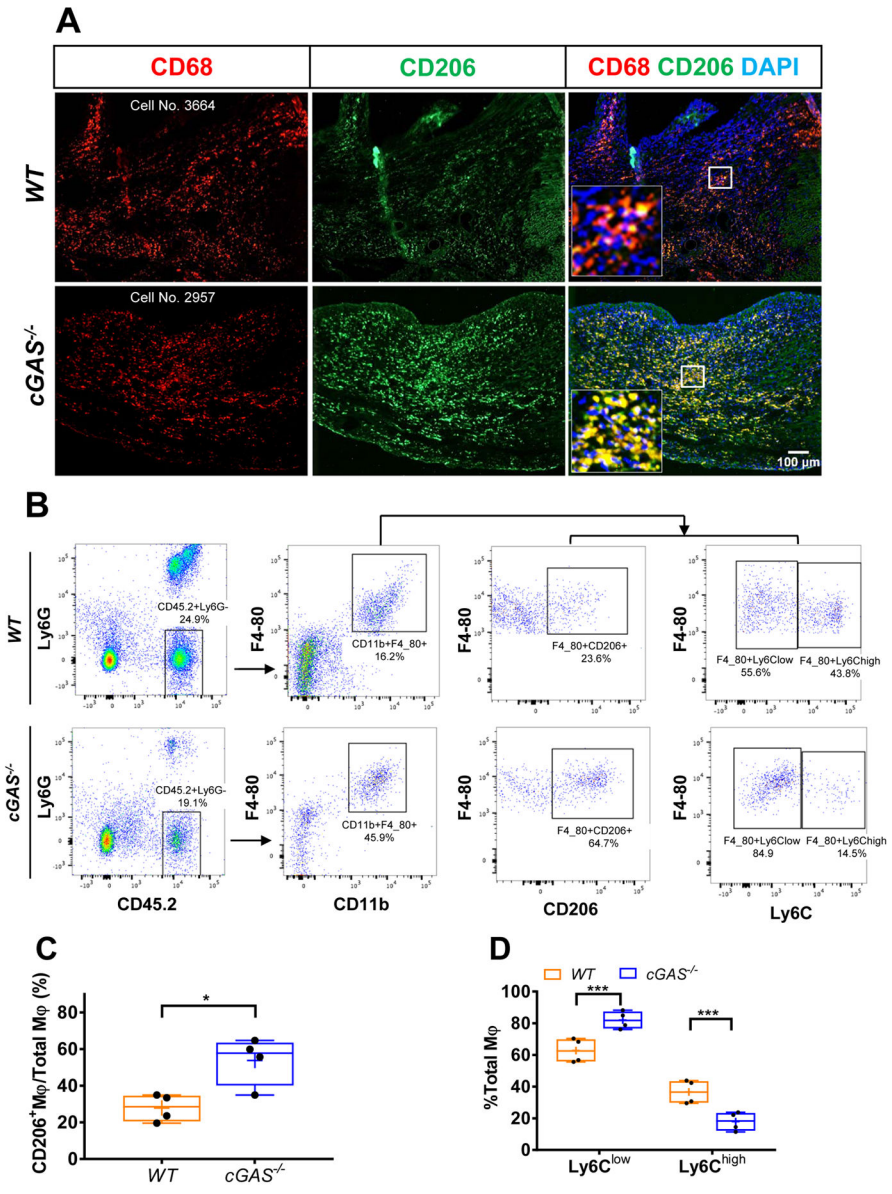

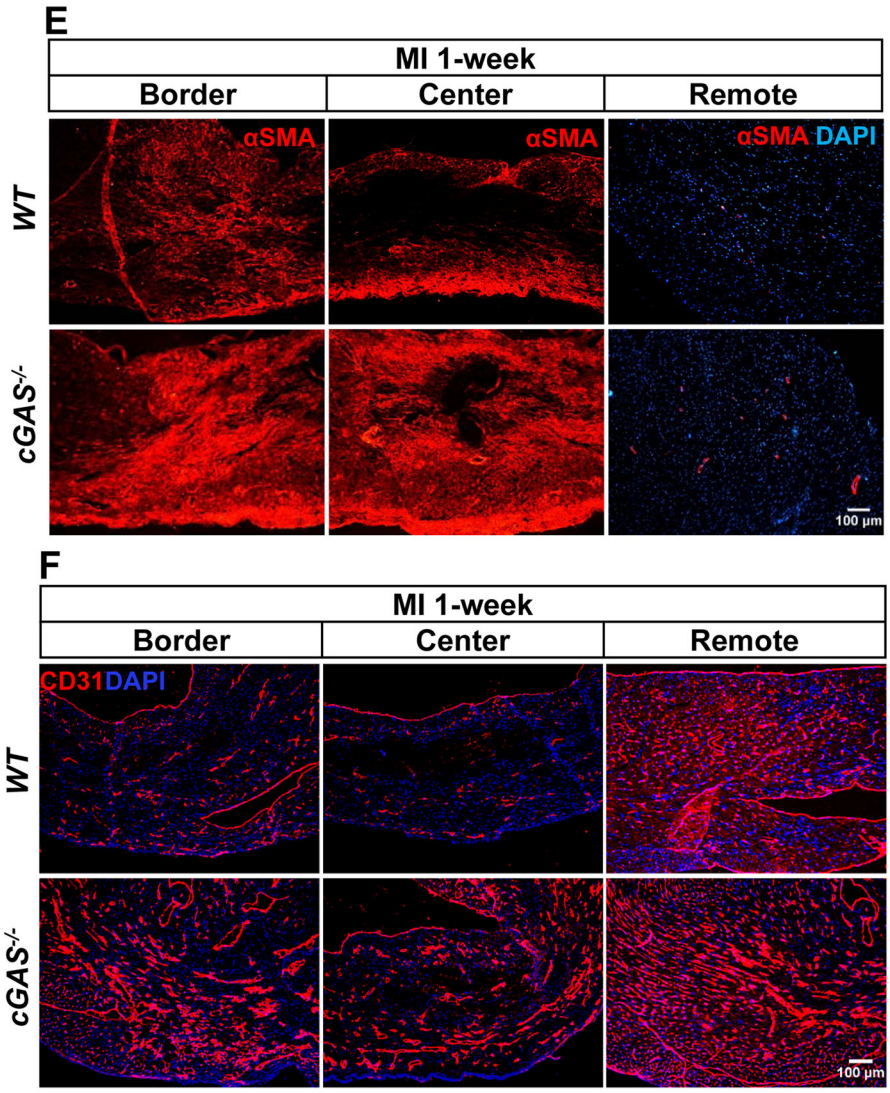

Figure 4. Silencing of cGAS-mediated cytosolic DNA sensing increases $CD68^{+}CD206^{+}$ (M2-like) macrophages and myofibroblasts in the region bordering the myocardial infarction

WT and *cGAS*$^{-/-}$ mice were subjected to LAD ligation. Six to seven days after surgery, hearts were perfusion-fixed with 4% PFA followed by cryosectioning at levels described in Methods. Alternatively, immune cells were isolated for FACS analysis. Scale bar: 100 μm. **A**. Heart sections co-labeled with CD68, a marker of total macrophages, and CD206, a marker of M2-like macrophages. **B.** Total, M1-like, and M2-like macrophages separated by FACS at post-MI day 7. **C and D**. Percentage of M1-like or M2-like cells in the ischemic tissue at post-MI day 6. **E**. MI hearts obtained from *WT* and *cGAS*$^{-/-}$ mice were stained with anti-αSMA. Images are from different areas of the infarct. **F.** Heart cryosections obtained from *WT* and *cGAS* null mice were stained with the endothelial marker CD31. Images acquired from the infarct center, infarct border, and remote areas. A cohort of 4–6 animals from *WT* or *cGAS*-null mice was evaluated for Figure 4. Box-and-whisker plots: the box extends from the 25th to 75th percentiles; whiskers depict minimal to maximal values; the mean is indicated as +. *p<0.05, **p<0.01, **p<0.001.

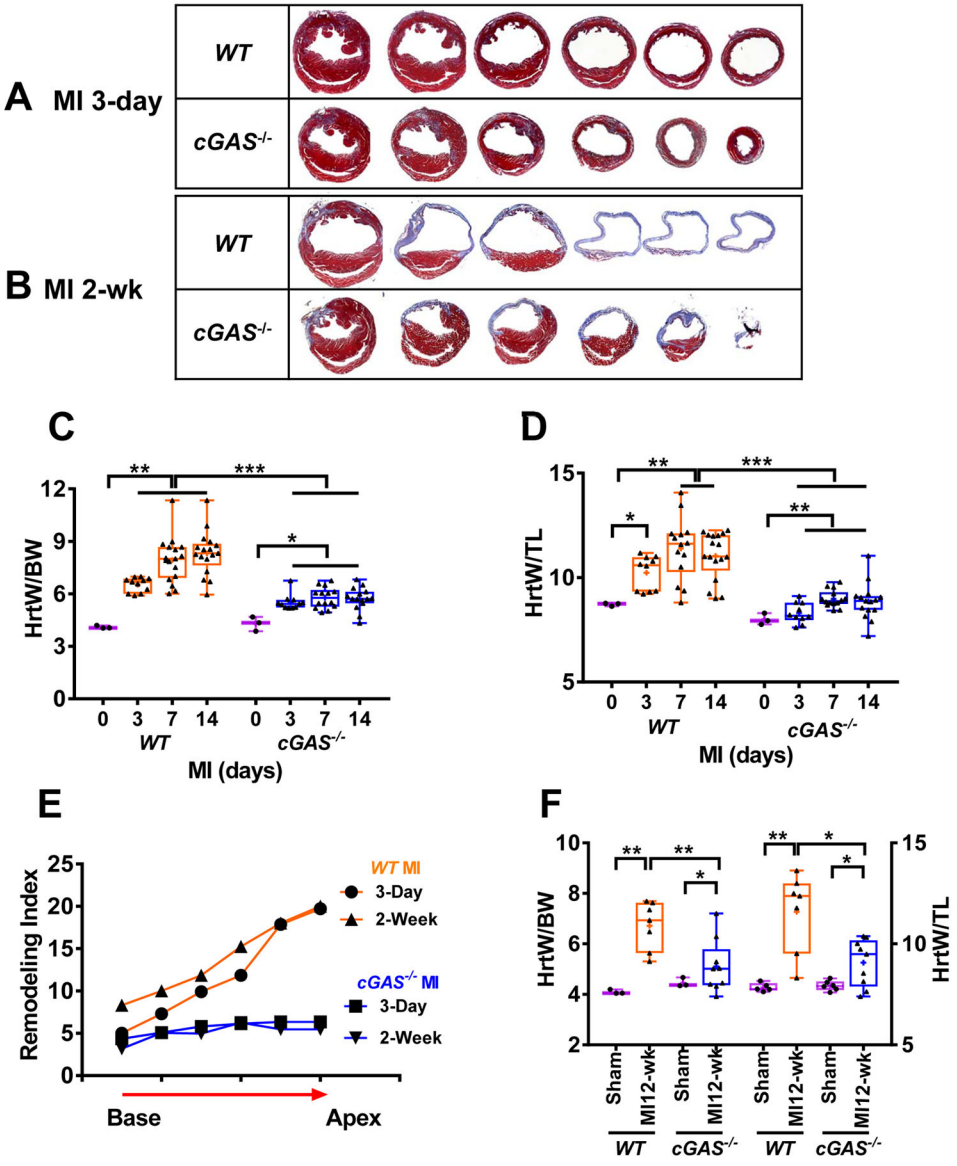

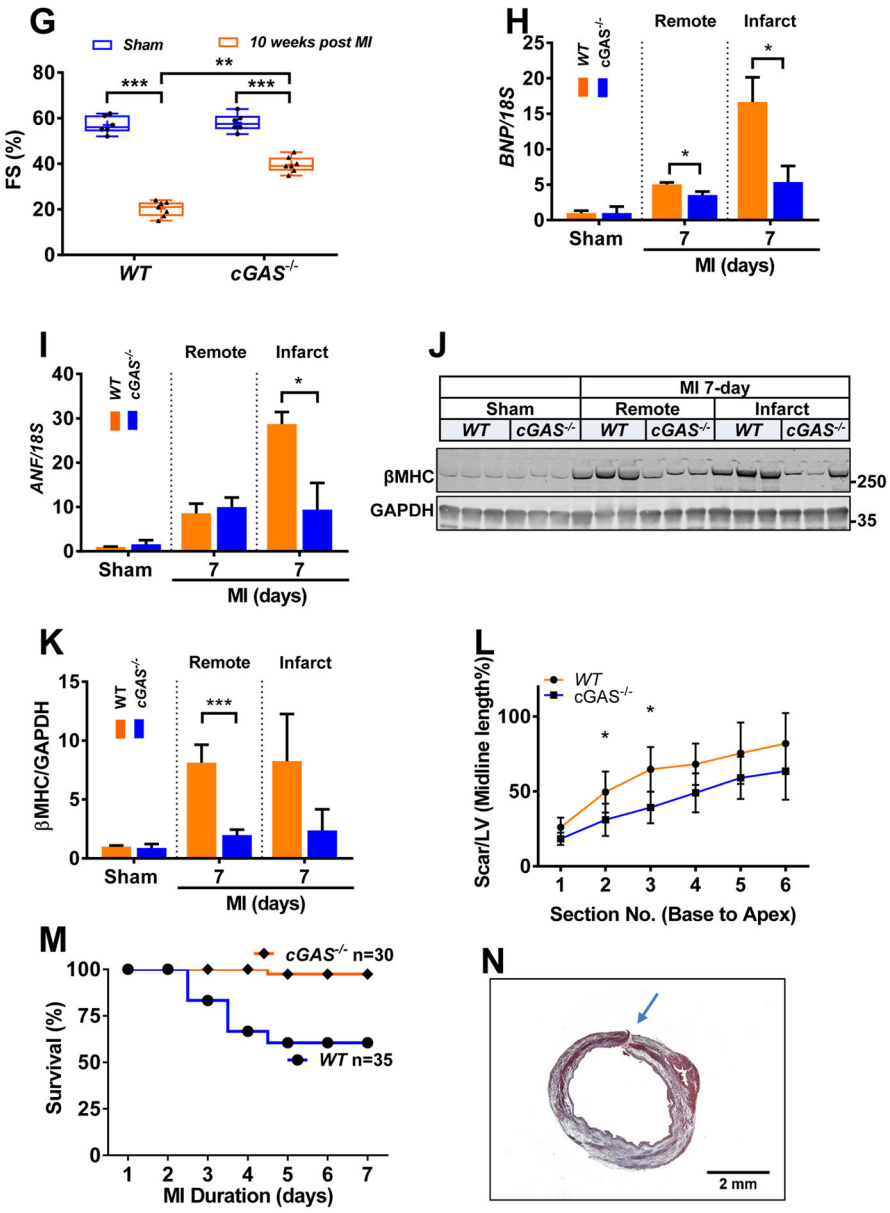

Figure 5. Silencing of cGAS-mediated cytosolic DNA sensing protects against MI-induced adverse ventricular remodeling and rupture

Short-axis sections of hearts post-MI. Sequential sections were obtained starting at the level of LAD suture and progressing toward the apex at 0.5 mm intervals at 3 days (**A,** n=6) and 14 days (**B,** n=11) post-MI. Scale bar: 2 mm. Increases in cardiac mass quantified as heart weight normalized to body weight (**C**) or tibia length (**D**). sham n=3; MI-3d n=10–11; MI-7d n=15–17; MI-14d n=15–17. **E**. Geometric remodeling index (GRI, LV cavity area/ septum thickness. *WT* n=6; cGAS-null n=11. **F.** Gravimetric analyses in the chronic remodeling phase 12 weeks post-MI. *WT* n=7; *cGAS*-null n=9 **G.** Contractile performance quantified as % fractional shortening 10 weeks post-MI. n=6–7. Activation of the fetal gene program measured as BNP (**H**), ANF (**I**), and βMHC (**J, K**). n=5–7. **L.** Percentage of midline scar length to LV circumference at MI-14d, quantified from sections obtained as

above in B, n=11. **M.** Post-MI survival. *WT* n=35; *cGAS*-null n=30. **N.** Representative example of ventricular rupture in a *WT* mouse heart 3 days after MI. Scale bar: 2 mm. Box-and-whisker plots: the box extends from the 25th to 75th percentiles; whiskers depict minimal to maximal values; the mean is indicated as +. *p<0.05, **p<0.01, **p<0.001.

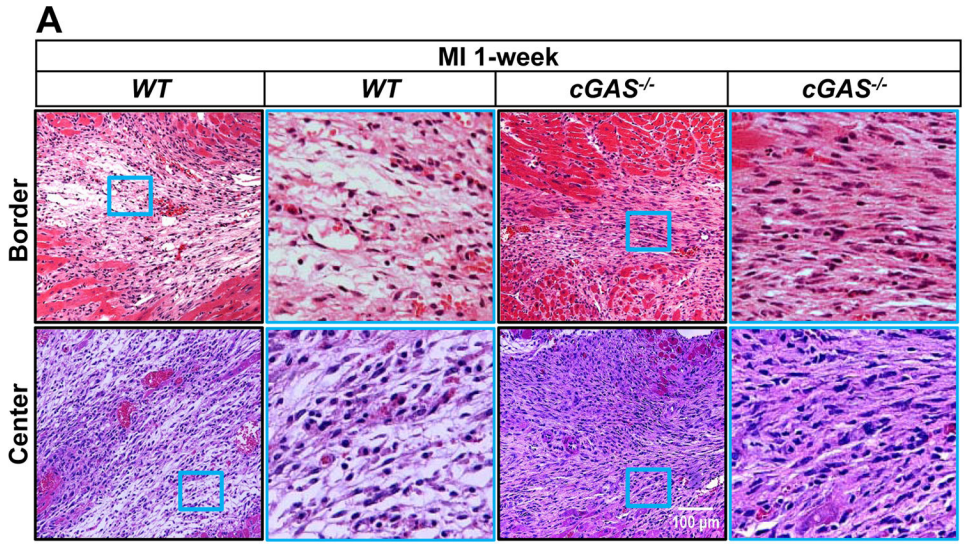

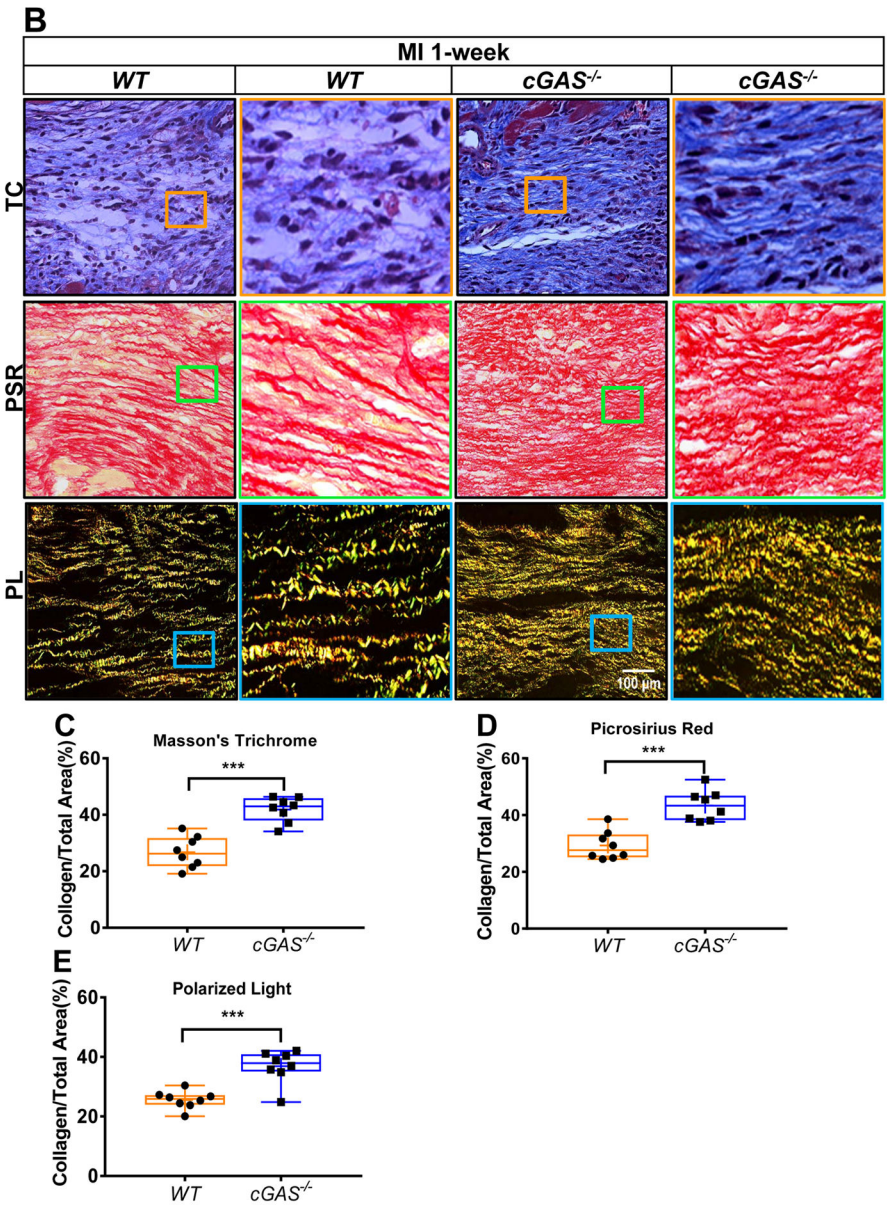

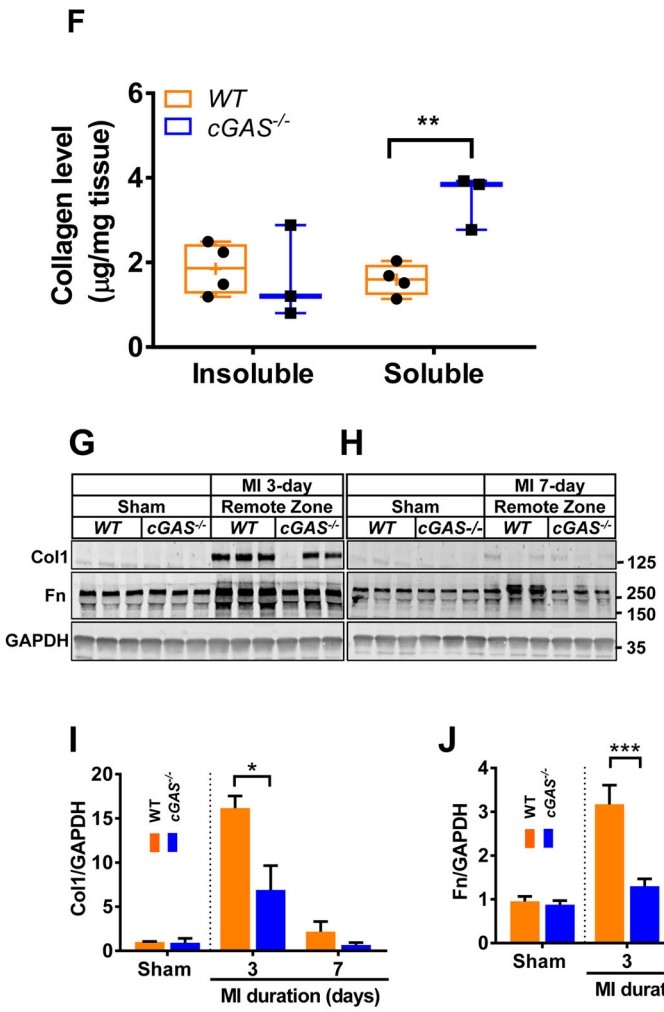

Figure 6. Silencing of cGAS enhances injury repair in the infarct region coupled with diminished ECM expansion in remote myocardium

WT and *cGAS*$^{-/-}$ mice were subjected to LAD ligation. One week after the procedure, hearts were harvested and fixed. Transverse sections were processed to obtain the following images. Scale bar: 100 μm throughout. **A.** H&E staining. **B.** Trichrome (TC) or picrosirius red (PSR) staining to detect collagen. Polarized light (PL) was used to examine collagen fiber structure. **C, D and E.** Collagen density quantified as the area of collagen divided by total area examined. **F**. Quantification of soluble and insoluble collagen purified from the infarct tissue at 1 week post MI. **G and H** Collagen and fibronectin proteins from the remote zone of myocardium as indicators of ECM expansion, a reflection of hemodynamic strain within those regions of ventricle. **I** and **J**. Summary data. n=4–10. Box-and-whisker plots: the box extends from the 25th to 75th percentiles; whiskers depict minimal to maximal values; the mean is indicated as +.*p<0.05, **p<0.01, **p<0.001.

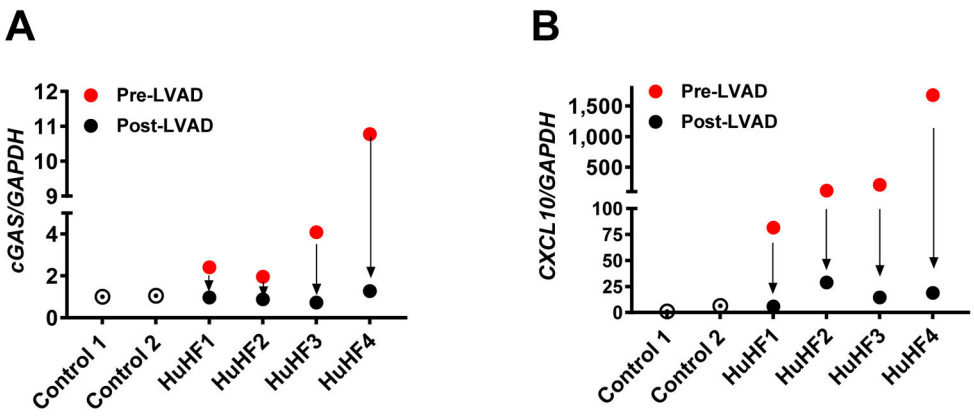

Figure 7. Dynamic changes in cGAS and CXCL10 in response to LV unloading in human heart failure

Total RNA was isolated from control human left ventricle, as well as paired ventricular tissues obtained before and after LVAD mechanical unloading. Quantitative RT-PCR was performed to quantify *cGAS* (**A**) and *CXCL10* (**B**) transcripts.

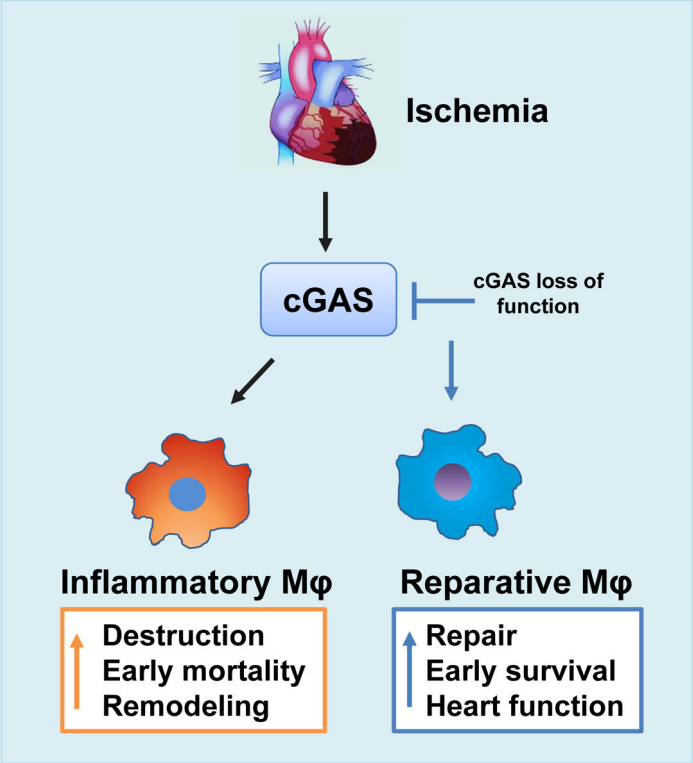

Figure 8. Model of cGAS-mediated cytosolic DNA sensing in post-infarction myocardial repair and remodeling

Ischemic injury activates cGAS-mediated signaling, possibly through detection and binding of nuDNA and mtDNA released from necrotic myocardium. cGAS activation promotes tissue destruction by sustaining pro-inflammatory macrophages (M1-like). Excessive tissue destruction leads to cardiac rupture, progressive remodeling, and heart failure. cGAS silencing promotes macrophage transformation toward a reparative (M2-like) phenotype that fosters efficient repair, mitigates adverse remodeling, and improves cardiac function.

Table 1

Baseline echocardiographic parameters in *WT* and *cGAS*-null mice.

ID	IVS;d	IVS;s	LVID;d	LVID;s	LVPW;d	LVPW;s	EF	FS	LV Mass	HR
	mm	**mm**	**mm**	**mm**	**mm**	**mm**	**%**	**%**	**mg**	**BPM**
WT1	0.98	1.65	2.31	0.97	0.72	1.49	89.76	58.10	54.57	714
WT2	0.98	1.61	3.15	1.47	0.80	1.57	85.38	53.33	93.05	693
WT3	1.21	1.69	2.96	1.26	0.95	1.63	88.66	57.39	114.35	707
WT4	1.01	1.72	2.95	1.16	0.75	1.60	90.72	60.68	83.15	739
Mean	1.04	1.67	2.84	1.22	0.80	1.57	88.63	57.38	86.28	713
SD	0.11	0.05	0.37	0.21	0.10	0.06	2.32	3.04	24.83	19
cGAS$^{-/-}$*1*	1.01	1.90	3.40	1.45	0.90	1.51	88.13	57.35	116.49	725
cGAS$^{-/-}$*2*	0.88	1.63	3.28	1.34	0.80	1.58	89.64	59.15	91.51	741
cGAS$^{-/-}$*3*	0.99	1.90	3.28	1.40	0.81	1.49	88.33	57.25	100.84	682
cGAS$^{-/-}$*4*	1.13	1.86	2.80	1.12	0.80	1.44	90.43	60.00	88.48	731
Mean	1.00	1.82	3.19	1.33	0.83	1.51	89.13	58.44	99.33	719
SD	0.10	0.13	0.27	0.15	0.05	0.06	1.09	1.36	12.59	26
P value	**0.62**	**0.07**	**0.18**	**0.41**	**0.69**	**0.16**	**0.71**	**0.55**	**0.38**	**0.70**

Table 2

Clinical characteristics of control subjects and heart failure patients.

Type	Etiology	Sex	Age	T2DM	HLD	HTN	CKD	COPD	Smoker
Control 1	NF	F	65	Yes	No	No	No	No	Former
Control 1	NF	F	55	Yes	No	Yo	No	No	Never
HuHF1	ICM	M	54	Yes	Yes	Yes	No	No	Former
HuHF2	ICM	M	64	Yes	Yes	Yes	Yes	Yes	Former
HuHF3	ICM	F	60	Yes	Yes	Yes	No	Yes	Former
HuHF4	ICM	M	56	Yes	Yes	No	Yes	No	Never